SIAMESE-RELATED1 Is Regulated Posttranslationally and Participates in Repression of Leaf Growth under Moderate Drought.

Marieke Dubois, Katia Selden, Alexis Bediée, Gaëlle Rolland, Nicolas Baumberger, Sandra Noir, Lien Bach, Geneviève Lamy, Christine Granier, Pascal Genschik

SIAMESE-RELATED1 Is Regulated Posttranslationally and Participates in Repression of Leaf Growth under Moderate Drought[1][OPEN]

Marieke Dubois,[a] Katia Selden,[b] Alexis Bediée,[c] Gaëlle Rolland,[c] Nicolas Baumberger,[a] Sandra Noir,[a] Lien Bach,[b] Geneviève Lamy,[a] Christine Granier,[c] and Pascal Genschik[a b,2]

[a]Institut de Biologie Moléculaire des Plantes, Centre National de la Recherche Scientifique, Unité Propre de Recherche 2357, Conventionné avec l'Université de Strasbourg, 67084 Strasbourg, France
[b]Biochimie et Physiologie Moléculaire des Plantes, Université de Montpellier, Centre National de la Recherche Scientifique, Institut National de la Recherche Agronomique, Montpellier SupAgro, 34060 Montpellier, France
[c]Laboratoire d'Ecophysiologie des Plantes sous Stress Environnementaux, Université de Montpellier, Institut National de la Recherche Agronomique, Montpellier SupAgro, 34060 Montpellier, France

ORCID IDs: 0000-0002-5190-2130 (M.D.); 0000-0002-5666-2885 (S.N.); 0000-0002-8853-5370 (G.L.); 0000-0002-4107-5071 (P.G.).

The plant cell cycle is tightly regulated by factors that integrate endogenous cues and environmental signals to adapt plant growth to changing conditions. Under drought, cell division in young leaves is blocked by an active mechanism, reducing the evaporative surface and conserving energy resources. The molecular function of cyclin-dependent kinase-inhibitory proteins (CKIs) in regulating the cell cycle has already been well studied, but little is known about their involvement in cell cycle regulation under adverse growth conditions. In this study, we show that the transcript of the CKI gene *SIAMESE-RELATED1* (*SMR1*) is quickly induced under moderate drought in young Arabidopsis (*Arabidopsis thaliana*) leaves. Functional characterization further revealed that SMR1 inhibits cell division and affects meristem activity, thereby restricting the growth of leaves and roots. Moreover, we demonstrate that SMR1 is a short-lived protein that is degraded by the 26S proteasome after being ubiquitinated by a Cullin-RING E3 ubiquitin ligase. Consequently, overexpression of a more stable variant of the SMR1 protein leads to a much stronger phenotype than overexpression of the native SMR1. Under moderate drought, both the *SMR1* transcript and SMR1 protein accumulate. Despite this induction, *smr1* mutants do not show overall tolerance to drought stress but do show less growth inhibition of young leaves under drought. Surprisingly, the growth-repressive hormone ethylene promotes *SMR1* induction, but the classical drought hormone abscisic acid does not.

In plants, organ development occurs postembryonically and requires accurate orchestration of cell divisions throughout the plant's life cycle (Gutierrez, 2005; De Veylder et al., 2007) by integrating endogenous signals and various cues from the environment (Inagaki and Umeda, 2011; Kitsios and Doonan, 2011). Whether cells divide or not is tightly controlled by more than 70 core cell cycle proteins (Van Leene et al., 2010). Cyclin-dependent kinases (CDKs) are key factors in triggering the different cell cycle steps (De Veylder et al., 2007; Harashima et al., 2013). A-type CDKs can associate with multiple cyclins (CYCs), including A-, B-, and D-type CYCs, and the CDKA/CYCD complex is crucial for progression into the S-phase and endoreplication (Boniotti and Gutierrez, 2001; Nakagami et al., 2002; Leiva-Neto et al., 2004; Nowack et al., 2012). The G2-M transition requires the formation of complexes of the plant-specific B-type CDK and CYCB (Harashima et al., 2013). Besides the binding with CYCs controlling their activity, plant CDKs are also subjected to regulation by interaction with CDK activating kinases and CDK inhibitory proteins (CKIs) (Komaki and Sugimoto, 2012; Kumar et al., 2015; Takatsuka et al., 2015).

Multiple CKI proteins function at the strictly controlled G1-to-S-phase and G2-to-M-phase transitions, where they bind to CDKs and block their activity. In Arabidopsis (*Arabidopsis thaliana*), the CKI group consists of 21 proteins divided in two subgroups: the KIP-RELATED PROTEIN group (KRP; 7 proteins) and the SIAMESE/SIAMESE-RELATED group (SIM/SMR; 14 proteins), which share a conserved CDK-inhibitory motif (Churchman et al., 2006; Kumar et al., 2015). KRP

[1] This work was supported by the Agence Nationale de la Recherche program "Programme Blanc ANR-12-BSV7-0021-02" and the LABEX program "ANR-10-LABX-0036_NETRNA."

[2] Address correspondence to pascal.genschik@ibmp-cnrs.unistra.fr.
The author responsible for distribution of materials integral to the findings presented in this article in accordance with the policy described in the Instructions for Authors (www.plantphysiol.org) is: Pascal Genschik (pascal.genschik@ibmp-cnrs.unistra.fr).

M.D., C.G., and P.G. designed the experiments; C.G. and P.G. supervised the experiments; M.D., K.S., A.B., G.R., N.B., S.N., and L.B. performed experiments; M.D., K.S., L.B., and G.L. generated plant material; M.D. and P.G. wrote the article with contribution of all the authors.

[OPEN] Articles can be viewed without a subscription.
www.plantphysiol.org/cgi/doi/10.1104/pp.17.01712

and SMR proteins regulate cell proliferation, organ size, and the timing of entry into endoreplication, a type of cell cycle in which the S-phase proceeds without M-phase, resulting in a doubling of the DNA amount (Wang et al., 2000; De Veylder et al., 2001; Coelho et al., 2005; Churchman et al., 2006; Roeder et al., 2010). *SMRs* also appear to have functions in specific cell types. For example, *SIAMESE* was discovered in a mutant that exhibited multicellular trichomes, due to a failure in restraining cell division (Walker et al., 2000). SMR family members have been found to bind CDKA and CDKB complexes, and their mode of action likely differs within the family: SIM, SMR1, and SMR2 would preferentially inhibit CDKB/CYCB complexes, while SMR4, SMR5, and SMR7 might block mainly CDKA/CYCD complexes (Walker et al., 2000; Van Leene et al., 2010). Intriguingly, SIM, SMR1, and SMR2 also have been shown to interact with CDKA/CYCD complexes, an observation that is not yet understood, since these CKIs do not seem to inhibit the S-phase (Churchman et al., 2006; Peres et al., 2007; Kumar et al., 2015).

In fungi and metazoans, the regulation of CKIs has been extensively studied and occurs not only at the transcriptional level, but also at the posttranslational level. CKIs are recognized and bound by E3 ubiquitin ligases and targeted for ubiquitin-mediated degradation by the 26S proteasome (Starostina and Kipreos, 2012; Genschik et al., 2014). In plants, our knowledge regarding posttranslational regulation of CKIs is limited to two members of the KRP family, KRP1 and KRP2, which are both targets of the 26S proteasome (Zhou et al., 2003; Verkest et al., 2005; Jakoby et al., 2006; Ren et al., 2008). The active domain is situated at the C terminus in both proteins and their N-terminal domain is necessary for mediating their degradation (Schnittger et al., 2003; Zhou et al., 2003; Jakoby et al., 2006). KRP2 degradation is likely initiated by CDKB1;1 phosphorylation and mediated by F-BOX PROTEIN-LIKE17 (FBL17) (Verkest et al., 2005; Noir et al., 2015), while KRP1 degradation might be mediated by other types of E3 ubiquitin ligases (Ren et al., 2008).

Interestingly, several *SMRs* were found to be transcriptionally induced in response to changing environmental conditions, leading to the hypothesis that *SMRs* may be involved in integrating environmental signals with cell cycle control (Peres et al., 2007; Yi et al., 2014; Kumar and Larkin, 2017). For instance, oxidative stress, as conferred by reactive oxygen species (ROS) or hydroxyurea, induces ROS production and *SMR4*, *SMR5*, and *SMR7* transcript levels, and *smr5* and *smr7* mutants are more tolerant to hydroxyurea treatments (Yi et al., 2014). Conversely, biotic stress imposed by *Pseudomonas syringae* infection suppressed *SMR1* expression, and *smr1* mutants are more susceptible to this bacterial infection (Hamdoun et al., 2016).

Of the abiotic stress conditions to which plants can be exposed, drought stress is one of the most deleterious (Araus et al., 2002). Drought stress is a complex stress that can occur at multiple levels of severity and cause specific damage at different stages of plant development. Moreover, drought often occurs in combination with other abiotic stresses such as heat. While severe drought stress affects the plant's energy metabolism by triggering stomatal closure, thereby reducing gas exchange and photosynthesis, plants responding to more moderate drought reduce shoot growth as an active mechanism to save water and energy resources (Claeys and Inzé, 2013; Verslues, 2017). At the cellular level, moderate drought stress quickly triggers the repression of cell expansion and cell division following the decrease in water availability (Harb et al., 2010; Baerenfaller et al., 2012; Bonhomme et al., 2012; Caldeira et al., 2014).

Several studies have pointed toward the possible functions of various plant hormones in this growth inhibition. Genes involved in the biosynthesis and signaling of abscisic acid (ABA), the classical drought hormone, are upregulated under drought stress in young, growing leaves, but also in mature leaves (Baerenfaller et al., 2012; Clauw et al., 2016). Notably, in actively growing leaves, no clear correlation was observed between the expression levels of these genes and the degree of growth reduction under drought (Clauw et al., 2016; Dubois et al., 2017). In contrast, the phytohormones ethylene, gibberellic acid, and jasmonic acid, which are typically involved in growth and defense responses, are emerging as possible regulators of growth under drought (Baerenfaller et al., 2012; Habben et al., 2014; Shi et al., 2015; Dubois et al., 2017). While these phytohormones might be implicated in the control of leaf growth and cell division under drought, the molecular mechanisms by which drought arrests the cell cycle currently remain uncharacterized.

In this study, we aimed to characterize how the plant cell cycle is affected at a molecular level in response to moderate drought stress. We found that the CKI protein SMR1 is transcriptionally induced and posttranslationally stabilized under moderate drought. We further characterized the regulation and function of SMR1 under both favorable growth conditions and drought stress using a multiscale approach.

RESULTS

SMR1 and *SMR5* Are Transcriptionally Induced by Moderate Drought

Drought is known to actively block Arabidopsis cell division, but it is still unclear which of the numerous CKIs might inhibit the cell cycle under drought. To identify candidate *CKI* genes under drought, we exposed Arabidopsis Col-0 plants to a moderate drought stress treatment using the automated watering platform PHENOPSIS (Granier et al., 2006) and quantified the transcript levels of all genes of the *KRP* and *SMR* families during leaf development (Fig. 1). Since drought stress is known to inhibit cell division within days following the watering arrest (Caldeira et al., 2014; Dubois et al., 2017), we paid particular attention to the genes

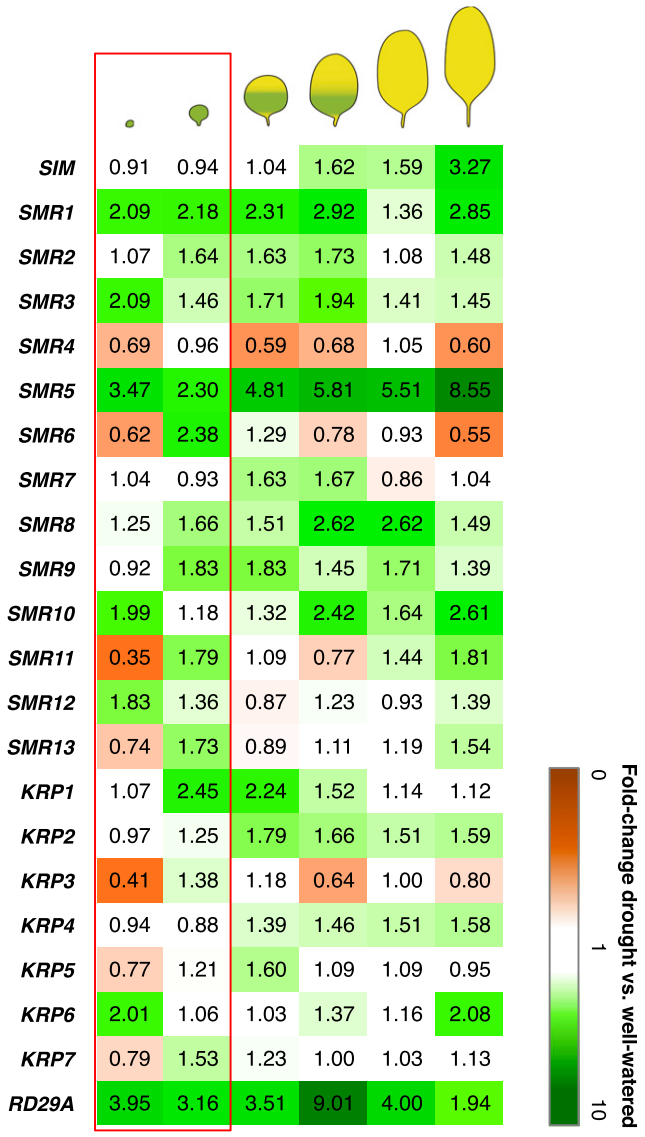

Figure 1. Transcript changes in *SMR* and *KRP* family genes under moderate drought stress. Drought stress was applied at the time of emergence of the sixth leaf, and expression levels of *SMR* and *KRP* genes were compared between well-watered and drought-stressed samples at different times during leaf development: proliferation phase (red box), expansion phase, and mature leaves (see "Materials and Methods"). Indicated values represent the fold change between drought and well-watered transcript levels. *RD29A* was used as a positive control for the drought stress treatment. Orange = down-regulation; green = up-regulation.

that responded to drought at the earliest harvested developmental time points, when the leaves were still fully in the proliferation phase (Fig. 1). Whereas none of the *KRP* gene family members responded clearly and rapidly to drought, two genes encoding SMR proteins, *SMR1* and *SMR5*, showed a pronounced induction by >2-fold upon moderate drought, which occurred quickly and was further maintained over time (Fig. 1). Because *SMR5* had previously been reported as being transcriptionally induced by a broad range of abiotic stresses (Peres et al., 2007; Yi et al., 2014), the observed induction might not necessarily reflect a specific role for SMR5 under drought. Moreover, the *SMR5* transcript level reached its highest up-regulation in full-grown leaves (Fig. 1), pointing toward a function that is most likely not restricted to the control of cell division under drought. We thus chose to focus further on *SMR1* in this study and hypothesized that it is potentially involved in arresting the cell cycle in Arabidopsis seedlings exposed to drought stress.

SMR1 Inhibits Cell Division, Thereby Restricting Growth of Roots and Leaves

Previous studies have reported a role for SMR1 in the control of cell divisions in Arabidopsis sepals and in trichome cells (Walker et al., 2000; Roeder et al., 2010), whereas its role in leaf growth is much less studied (Kumar et al., 2015). To investigate the possible functions of SMR1 in root and shoot growth, we first phenotypically characterized an *smr1* loss-of-function mutant. For root growth analysis, the mutant and the appropriate wild type were grown in vitro and the primary root length was measured at 12 d after stratification (DAS). In *smr1*, the primary root showed a mild but reproducible increase in length by 9% (P = 2.2E-11; $ANOVA_{TukeyHSD}$; Fig. 2A). For rosette analysis, we measured total rosette area and individual leaf size after 3 weeks of growth in soil, before the plants started bolting. No difference in total rosette area was observed between the wild type and *smr1* mutants (Supplemental Fig. S1), as previously reported (Kumar et al., 2015). Notably, a detailed analysis of the area of each individual leaf of the rosette revealed an increase in leaf size of the oldest leaves, with a reproducible increase in area of the second leaf by 21% (P < 1E-10; $ANOVA_{TukeyHSD}$) in *smr1* compared with wild-type plants (Fig. 2B).

Although the effects of SMR1 loss of function at the whole-plant level are subtle, more pronounced effects were observed at cellular level. In the root tip, the length of the cell division zone increased by 30% (P = 9.5E-15, $ANOVA_{TukeyHSD}$) in *smr1* mutants (Fig. 2C; Supplemental Fig. S2). In a full-grown sixth leaf, we found a strong increase (by 84%, P = 1.9E-8, Student's t test) in the number of adaxial epidermal cells in the *smr1* mutant (Fig. 2D). This was accompanied by a severe reduction in cell size (−40%, P = 8.6E-9, Student's t test), which explains the absence of a clear effect at the level of the leaf. Subsequent cellular analysis over time during leaf development showed that this cellular phenotype arises very early during development and further increases over time (Supplemental Fig. S3). These cellular results suggest that SMR1 might control the switch from cell division to cell expansion during root and leaf growth. To further investigate this possibility, we visualized the *SMR1* expression pattern using the *pSMR1::GUS* line that was described previously

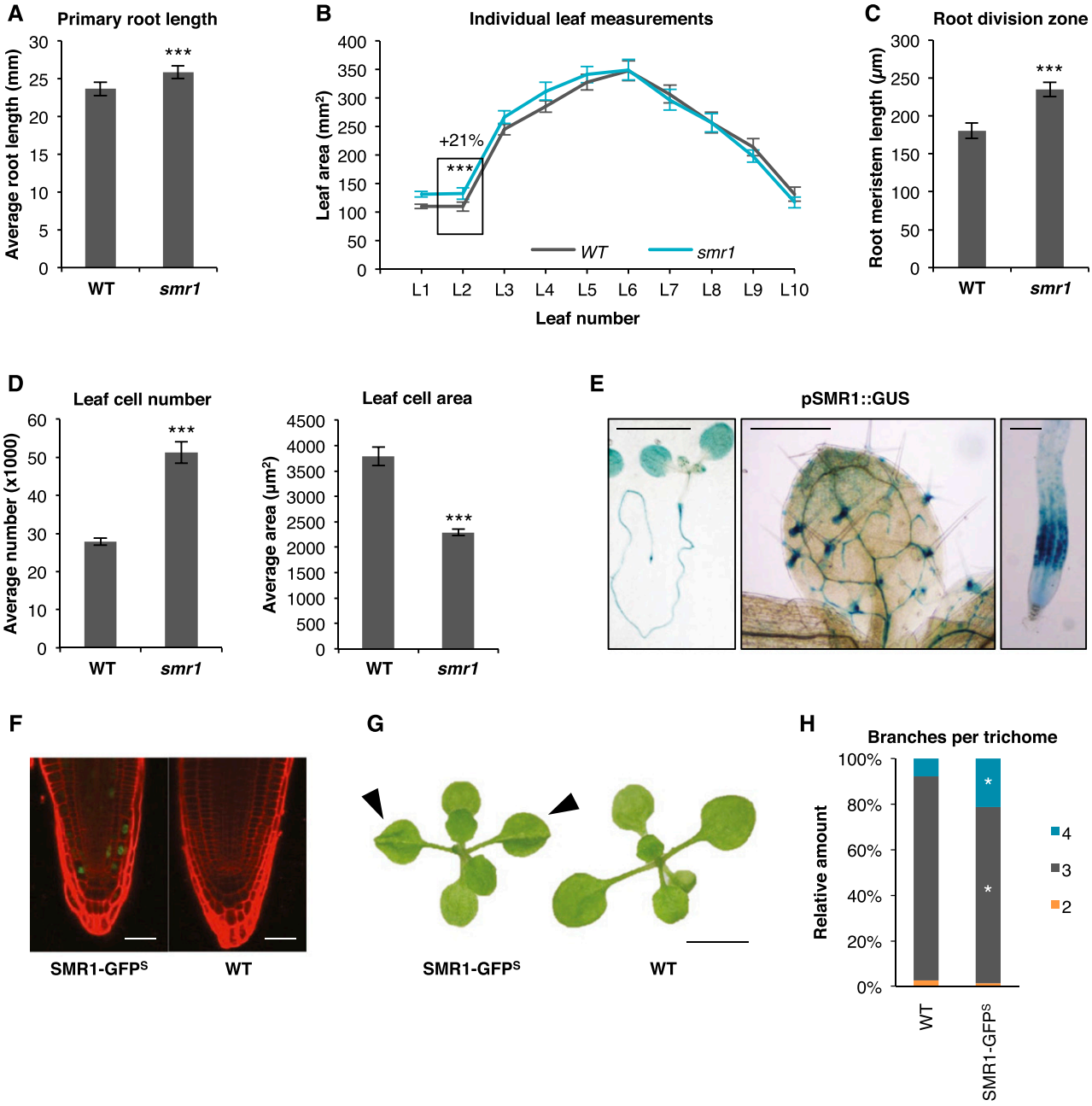

Figure 2. Phenotypic analysis of *smr1* mutants and SMR1-GFP overexpression lines. A, Root length of the *smr1* mutants after 12 d of growth in vitro. Mean ± SE, $n = 3$ biological repeats, with 50 plants per line per repeat, $^{***}P < 0.001$, ANOVA. B, Area of each individual leaf (L1–L10) of *smr1* after 22 d of growth in soil with manual watering. Mean ± SE, $n = 3$ biological repeats, with 10 plants per line per repeat, $^{***}P < 0.001$, $\text{ANOVA}_{\text{TukeyHSD}}$. C, Root meristem length of plants as described in A, measured as the length between the quiescent center and the last dividing cell of the cortex (Supplemental Fig. S2). Mean ± SE, $n = 3$ biological repeats, with > 12 plants per line per repeat, $^{***}P < 0.001$, ANOVA. D, Cellular analysis of adaxial epidermis cells of *smr1* leaves at maturity. Mean ± SE, $n = 12$ leaves, $^{***}P < 0.001$, Student's *t* test. E, GUS pattern of the pSMR1::GUS promoter-reporter line, visualized after 9 d of in vitro growth. Scale bar represents (from left to right) 5 mm, 500 µm, and 100 µm. F, Root tip of SMR1-GFP^S overexpression line and wild-type seedling imaged after 9 d of growth in vitro. Scale bar = 25 µm. G, Fifteen-day-old SMR1-GFP^S overexpression line and wild-type seedling. Arrows highlight cup-shaped leaves. Scale bar = 5 mm. For E to G, representative seedlings are shown. H, Trichome branching patterns in the SMR1-GFP^S overexpression line, measured on leaf 2 of 15-d-old seedlings; >25 trichomes per leaf, 8 plants per line, $^{*}P < 0.05$, Student's *t* test.

(Yi et al., 2014). *SMR1* was predominantly expressed in the transition zone of the root tip where dividing cells start to expand (Fig. 2E). In very young leaves, where cells switch from cell cycle to endoreplication and differentiation in a gradient from the tip to the base of the leaf, *SMR1* is mainly expressed in the leaf tip where

cells stop dividing (Fig. 2E). Notably, we also observed dots of GUS staining in the leaves, corresponding to trichome cells (Fig. 2E).

Finally, to further confirm these observations and characterize SMR1 at a molecular level, we generated stable Arabidopsis lines expressing GFP-tagged SMR1 under the control of either the endogenous promoter (*pSMR1::SMR1-GFP*) or the CaMV 35S promoter (*p35S::SMR1-GFP*). For the latter, two independent transgenic lines with strong (S) or weak (W) overexpression levels were generated and were called SMR1-GFP^S and SMR1-GFP^W, respectively. Introgression of the SMR1-GFP^W constructs in the *smr1* mutant background rescued the cellular *smr1* phenotype, validating the functionality of the fusion constructs and the specificity of the *smr1* mutant (Supplemental Fig. S4). For all tested lines, the fusion protein localized exclusively to the nucleus (Fig. 2F; Supplemental Fig. S5) as predicted by the PredictNLS nuclear localization signal detection tool (Rost and Liu, 2003). At the phenotypic level,SMR1-GFP^W and *pSMR1::SMR1-GFP* plants did not show obvious visible phenotypes, in terms of rosette and root size, or trichome development. In contrast, plants overexpressing SMR1-GFP^S were smaller and had cup-shaped rosette leaves (Fig. 2G; Supplemental Fig. S6). Compared to the wild type, the leaves of SMR1-GFP^S plants had trichomes with an increased number of branches (Fig. 2H). In the root apical meristem, the meristematic structure was clearly affected in SMR1-GFP^S: the cell division zone was reduced because root cells close to the quiescent center sporadically started to expand prematurely, coinciding with the appearance of the SMR1-GFP fusion protein (Fig. 2F). Together, these results showed that SMR1 reduces cell division in roots and leaves and pushes dividing cells toward expansion, which ultimately leads to a mild effect on root and leaf growth.

SMR1 Interacts with CDKA without Inhibiting the Transition to S-Phase

In order to further understand the function of SMR1 at a molecular level, we investigated at which phase(s) of the cell cycle SMR1 could exert its CDK-inhibitory function. We first tested which CDK protein could physically interact with SMR1 by performing coimmunoprecipitation assays on the SMR1-GFP protein in the SMR1-GFP^S Arabidopsis line treated with MLN4924 to stabilize protein complexes. Upon immunoprecipitation of the SMR1-GFP complexes, both CDKA and CDKB reproducibly coimmunoprecipitated (Fig. 3A). While the SMR1/CDKB complex was expected (Van Leene et al., 2010), the interaction with CDKA was more surprising. Conversely, by pulling down CDKA with p9^{CKS1} affinity beads (De Veylder et al., 1997; Dissmeyer and Schnittger, 2011), we reproducibly coprecipitated SMR1-GFP (Fig. 3B). To further confirm this SMR1/CDKA interaction, we transiently expressed SMR1-GFP and CDKA-RFP in *Nicotiana benthamiana* leaves and performed fluorescence lifetime imaging-fluorescence resonance energy transfer (FLIM-FRET) with SMR1-GFP as the energy donor and CDKA-RFP as receptor. In the nucleus, where both fusion proteins localize (Supplemental Fig. S7), we measured 18.3% ($P < 1E\text{-}7$; $ANOVA_{TukeyHSD}$) energy transfer from SMR1-GFP to CDKA-RFP, validating the existence of SMR1/CDKA complexes (Fig. 3C).

Since CDKA is primarily required for entry into S-phase (Nowack et al., 2012), binding by SMR1 could point toward an inhibition of the S-phase by SMR1. To test this possibility, we measured the ploidy levels in young leaves of *smr1* and SMR1-GFP^S plants. While *smr1* mutants showed overall slightly lower ploidy levels than the wild type, nuclei of SMR1-GFP^S leaves contained higher DNA amounts (Fig. 3D). This tendency appeared already very early during leaf development, when cells are still actively dividing (Fig. 3D, 9DAS), suggesting that SMR1 negatively affects the transition to M-phase. Together, these results confirm that SMR1 pushes dividing cells out of the mitotic cell cycle toward endoreplication, despite its interaction with CDKA.

We next investigated whether SMR1 itself might be regulated by the interaction with CDKA. In mammals, CKIs have been shown to be targeted for posttranslational degradation upon phosphorylation by CDK2 proteins, the orthologs of plant CDKA (Sheaff et al., 1997), and similar mechanisms have been observed for KRP2, which is phosphorylated by CDKB1;1 prior to degradation (Verkest et al., 2005). While such posttranslational regulatory mechanisms have not been reported for SMR family proteins so far, an amino acid sequence comparison between SIM and SMR1 highlighted a putative CDKA phosphorylation site at the SMR1 N terminus (Churchman et al., 2006). In-depth sequence analysis of all SMRs revealed a similar domain (S/T-P-X-K/R) in the SMR5 N terminus, while SMR9, SMR10, and SMR12 also carry this domain in their C termini as part of the conserved Motif #1 (Supplemental Fig. S8). We thus asked whether the putative CDKA phosphorylation site in SMR1 is important for the stability of the SMR1 protein, as is the case for KRP2 upon CDKB phosphorylation. We generated a 35S::SMR1$^{\Delta TPIK}$-GFP variant of SMR1 in which the S/T-P-X-K/R-motif for CDKA phosphorylation was deleted and expressed it in *N. benthamiana* leaves, together with SMR1-GFP. Subsequently, further translation was blocked by addition of the drugs cycloheximide (CHX) and the SMR1-GFP and SMR1$^{\Delta TPIK}$-GFP protein levels were monitored. We observed a decrease in SMR1-GFP levels, and, interestingly, this degradation was slightly but reproducibly less pronounced for SMR1$^{\Delta TPIK}$-GFP (Fig. 3E). These results indicate that the putative CDKA phosphorylation site likely contributes to SMR1 protein turnover but that its mutation is not sufficient to abolish SMR1 degradation.

SMR1 Is a Short-Lived Protein Degraded by the Proteasome

The experiment described above suggested that SMR1 may be posttranslationally regulated. We

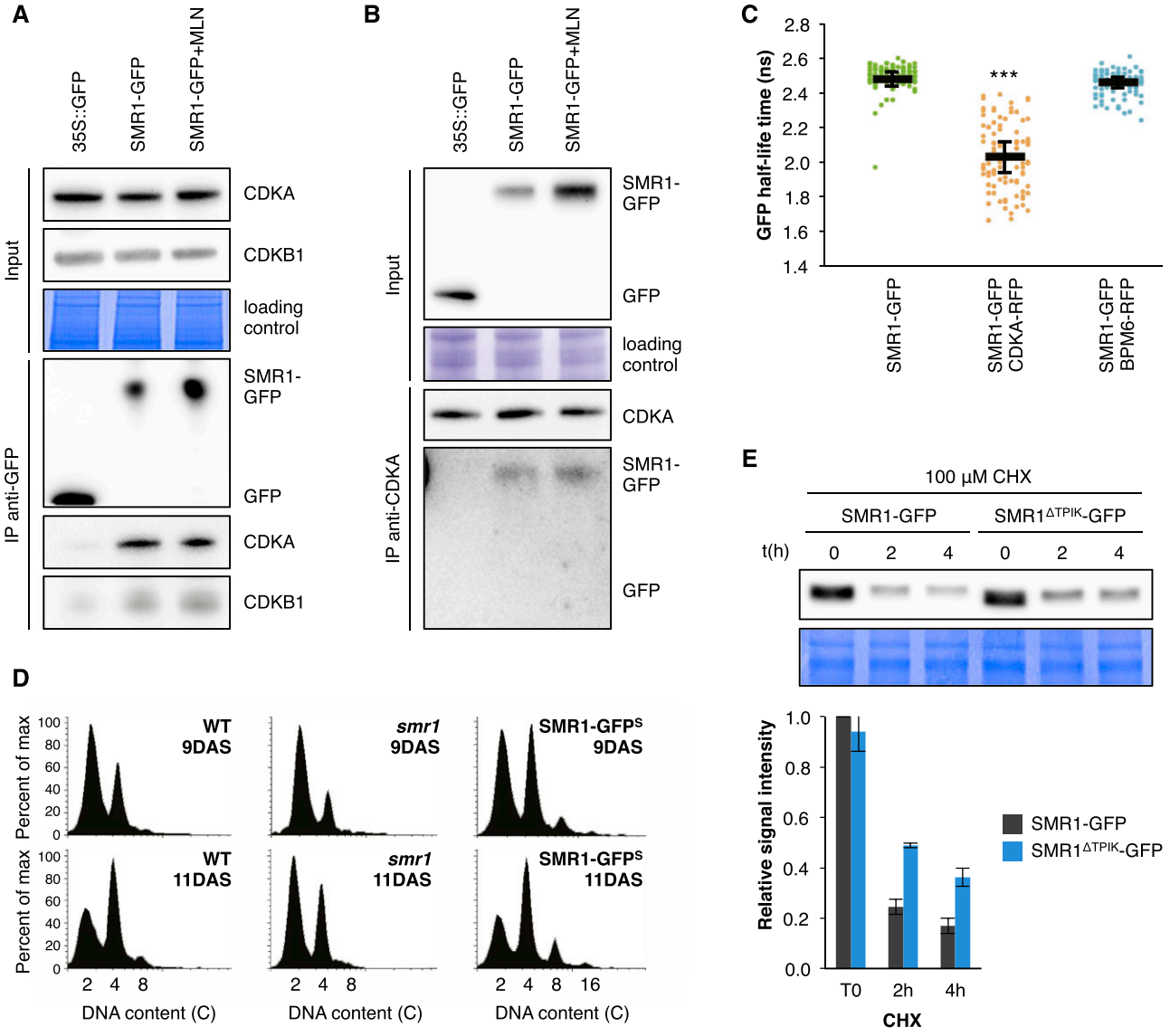

Figure 3. Molecular and functional interactions between SMR1 and CDKA. A, Immunoprecipitation of GFP- and SMR1-GFP-bound protein complexes, without and with addition of MLN4924 to stabilize protein complexes, followed by detection of CDKA and CDKB1. B, Reverse pull-down of CDKA-bound complexes using $p9^{CKS1}$ affinity beads followed by detection of GFP and SMR1-GFP. C, Analysis of SMR1/CDKA interaction by FLIM-FRET in *N. benthamiana* leaves. The nuclear protein BPM6-RFP was used as a negative control (Lechner et al., 2011). Mean ± SE, $n = 2$ biological repeats, with > 30 nuclei per repeat, $^{***}P < 0.001$, $ANOVA_{TukeyHSD}$. D, Ploidy levels in the *smr1* mutant, $SMR1\text{-}GFP^S$ overexpression line, and the wild type. DNA contents were measured in the second leaf at 9 and 11 DAS. E, Protein degradation assay of SMR1-GFP and $SMR1^{\Delta TPIK}$-GFP, in which the putative CDKA-phosphorylation site of SMR1 has been deleted. Proteins were expressed transiently in *N. benthamiana* leaves treated with 100 μM CHX. The quantification (bottom panel) represents the mean ± SE of 2 biological repeats.

intended to further explore this in stable Arabidopsis lines and therefore treated 1-week-old SMR1-GFP transgenic plants with CHX. We observed an abrupt decrease in SMR1-GFP levels, with an average half-life time of 30 min in both independent transgenic lines (Fig. 4A; Supplemental Fig. S9). Upon 4 h of treatment, the pool of SMR1-GFP was mostly degraded (Fig. 4, A and B). In eukaryotes, selective protein degradation mainly occurs through ubiquitylation of the target protein by an E3 ubiquitin ligase, followed by degradation through the 26S proteasome (Vierstra, 2009). To further investigate whether SMR1 protein degradation occurs through this pathway, we performed treatments with MG-132 or MLN4924, drugs that block the proteasome and inhibit neddylation of Cullin-RING type E3 ubiquitin-ligases (CRLs), respectively. Both drugs clearly prevented the degradation of SMR1 (Fig. 4B), suggesting that SMR1 is ubiquitylated by a CRL-type E3 ubiquitin ligase and subsequently degraded by the 26S-proteasome.

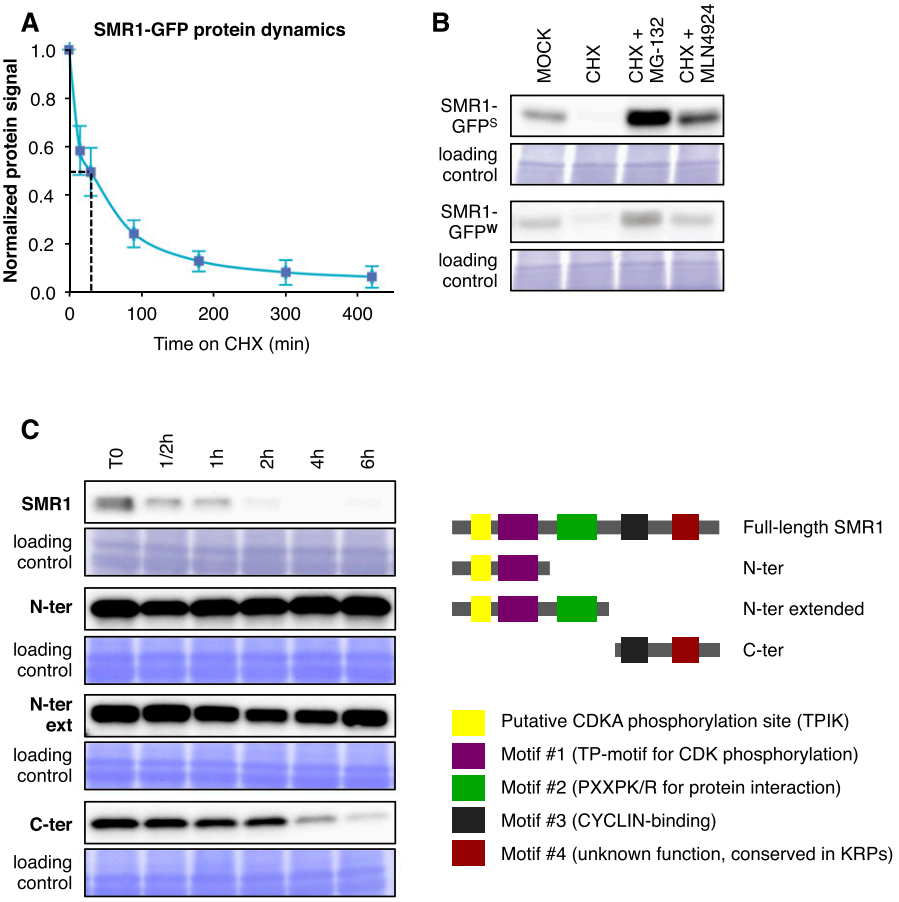

Figure 4. Analysis of SMR1 protein stability. A, SMR1-GFP protein levels in the SMR1-GFPS transgenic line over time upon treatment with 100 μM CHX. The intensity of the SMR1-GFP protein signal was normalized to the intensity of the loading control (Coomassie blue staining) and subsequently expressed relatively to the normalized signal at T0. The dotted line indicates the time at which the SMR1-GFP protein level was reduced by half (half-life). Mean ± SE, n = 3 biological repeats. B, SMR1-GFP protein levels in the SMR1-GFP transgenic lines upon 4 h of treatment with CHX alone or in combination with the proteasome-inhibitory drug MG-132 or the neddylation inhibitor MLN4924 blocking CRL-type E3-ligases. C, Stability of the truncated variants of SMR1 upon inhibition of translation by CHX in *N. benthamiana* leaves. See also Supplemental Figure S10.

In plants, very little is known about E3 ubiquitin ligases controlling CKI degradation. We have previously shown (Noir et al., 2015) that the Arabidopsis FBL17 protein plays an important role in leaf development and cell division and is involved in the degradation of the CKI KRP2. Since the *fbl17* phenotype resembles that of seedlings strongly accumulating SMR1-GFP, FBL17 is a candidate F-box protein that may direct SMR1 degradation. To investigate this, we introgressed the *SMR1-GFP*^{S} construct in the *fbl17* mutant background and selected 8-d-old *fbl17* mutants as explained by Noir et al. (2015). Surprisingly, the SMR1-GFP protein was not stabilized in *fbl17* but was almost completely degraded (Supplemental Fig. S9). Interestingly, we noticed an increase in CDKA protein levels in the *fbl17* mutant (Supplemental Fig. S9). These observations thus show that FBL17 is not the F-box protein directly targeting SMR1 for degradation, but further support the hypothesis that CDKA could be involved in SMR1-GFP degradation.

Besides the putative CDKA phosphorylation domain, SMR1 contains four well-conserved domains, some of which have unknown functions (Kumar et al., 2015; Supplemental Fig. S8). To get further insights in SMR1 protein turnover, we tested whether one of these domains was important for SMR1 stability. We first generated truncated SMR1 proteins for GFP-fusions: the N-terminal region carrying Motif #1, an extended N-terminal region containing Motifs #1 and #2, and the C-terminal region containing Motifs #3 and #4 (Fig. 4C). Subsequently, protein decay was assayed in *N. benthamiana* leaves as described above. For all truncated proteins, we observed a reproducible overall increase in protein level as compared to the full-length SMR1 (Fig. 4C). Both truncated proteins containing only the N-terminal region of SMR1 were stable even in the presence of CHX. In contrast, the C-terminal region of SMR1 could be degraded, though less efficiently than the full-length protein (Fig. 4C). Interestingly, the SMR1 C-terminal domain could still interact with CDKA in the FLIM-FRET assay (Supplemental Fig. S10A). At the cellular level, we observed altered localization of the truncated protein containing the N-terminal region, which localized mainly to the cytosol (Supplemental Fig. S10B). The C-terminal region of SMR1 localized exclusively in the nucleus, as did the full-length SMR1. Together, these results show that the C terminus of SMR1 interacts with CDKA, is crucial for the nuclear localization, and is mostly, but not solely, responsible for SMR1 turnover. Therefore, it is likely that additional

elements are present in the N terminus of SMR1, such as the CDKA phosphorylation site described above, which might also participate in SMR1 degradation.

The Lys-Less SMR1 Protein Is More Stable and Still Functional

Next, we investigated the physiological importance of SMR1 protein degradation and aimed to generate transgenic Arabidopsis lines expressing nondegradable SMR1 alleles. Since ubiquitylation of proteins generally occurs on Lys (K) residues, the SMR1 protein sequence was modified by replacing all lysines with arginines (R). The Lys-less $SMR^{K>R}$-GFP variants were expressed under the control of the CaMV 35S promoter and we selected two independent transgenic lines, $SMR^{K>R}$-GFP^1 and $SMR^{K>R}$-GFP^2, for which the homozygous plants had a transcript level similar to the SMR1-GFP^S line (Fig. 5A). Despite the comparable SMR1 transcript levels in SMR1-GFP^S and $SMR1^{K>R}$-GFP lines, the $SMR1^{K>R}$-GFP transgenic lines accumulated between two and four times more fusion protein (Fig. 5A; Supplemental Fig. S9). When the translation of new proteins was inhibited with CHX, the half-life of $SMR1^{K>R}$-GFP proteins was 75 min on average, compared to 30 min for the SMR1-GFP (Fig. 5B). This decrease in SMR1 protein turnover rate could explain why the $SMR1^{K>R}$-GFP proteins are more abundant in the transgenic lines than their nonmutated homologs (Supplemental Fig. S9). The $SMR1^{K>R}$-GFP degradation was fully blocked in the presence of MLN4924 and MG-132, indicating that additional residues beside Lys can serve as acceptors of ubiquitin (Supplemental Fig. S11).

When propagating the $SMR1^{K>R}$-GFP transgenic plants, we did not succeed in obtaining a homozygous T3 population. Plants homozygous for $SMR1^{K>R}$-GFP were extremely dwarfed and failed to reach the reproductive growth stage (Fig. 5C). Similarly, root length was severely reduced by 70% (Fig. 5D), and the root apical meristem was completely unstructured (Fig. 5E). Plants heterozygous for the construct, which were viable and fertile, also showed a clear reduction in root length and leaf size, as well as pronounced leaf serrations (Fig. 5, C and D). In addition, the adaxial trichomes of $SMR1^{K>R}$-GFP plants possessed more branches than wild-type or SMR1-GFP^S plants, with trichomes developing up to five branches (Fig. 5F; Supplemental Fig. S12A). Finally, $SMR1^{K>R}$-GFP leaves showed even higher endoreplication levels than SMR1-GFP^S leaves (Supplemental Fig. S12B). Together, these results show that the Lys-less variants of SMR1 are functional proteins, which exacerbate the defects from *SMR1* overexpression due to their increased stability.

smr1 Mutants Show Less Growth Inhibition under Moderate Drought

A prompt decrease in leaf growth is among the first reactions to drought stress in plants (Caldeira et al., 2014), and notably, CDKA activity has previously been shown to decrease in the presence of osmotic stress (Skirycz et al., 2011a). Based on the interaction between SMR1 and CDKA, the possible involvement of the CDKA kinase in SMR1 protein stability, and the observation that *SMR1* is transcriptionally responsive to drought, we investigated whether SMR1 would inhibit growth under water-limited conditions. We developed a moderate drought stress assay focusing on the second leaf, which showed the most pronounced phenotypic difference in *smr1* under control conditions (Fig. 2B). In the drought setup, water was first withheld when the second leaf emerged from the shoot apical meristem, then expression, protein abundance, and leaf area measurements were performed within a time frame of days upon water withholding to increase the probability of observing direct effects rather than long-term acclimatization mechanisms. We first confirmed that with this setup *SMR1* was transcriptionally induced in the shoot, and particularly in young leaves (Fig. 6A). Because SMR1 is also regulated at the posttranslational level (see above), we verified that SMR1-GFP protein accumulates upon drought. In the second leaf, SMR1-GFP protein levels increased upon drought treatment, which was most pronounced at the earliest measured time point after drought onset (Fig. 6B). These observations show that *SMR1* is transcriptionally induced and that SMR1 remains stable under short-term drought stress.

Next, *smr1* mutants were exposed to moderate drought treatment. In the first attempt, we applied a long-term drought treatment and measured rosette size at maturity. Under these conditions, the *smr1* mutant was equally sensitive to drought as the wild type, with drought-induced size reductions of 51% and 56%, respectively (Fig. 6C). Reasoning that a potential difference in cell division arrest might be masked by compensatory mechanisms when the drought treatment persists for weeks, we subsequently scored short-term drought sensitivity by measuring the area of the actively growing second leaf after 8 d of water limitation. In these assays, the leaf area of wild-type plants was reduced by an average of 41.2%. In contrast, *smr1* mutants showed a less pronounced drought-induced growth inhibition, with relative reductions in leaf area of 23.8% ($P_{TREATMENT*GENOTYPE}$ = 3.1E-15; ANOVA; Fig. 6D). Together, these data show that SMR1 participates in leaf growth inhibition of plants exposed to short-term moderate drought stress. This tendency is specific for young, actively growing leaves and disappears when leaves get older, when the applied drought stress was more long-term.

Upstream, Ethylene Induces *SMR1* Expression, But ABA Does Not

To further explore *SMR1* transcriptional induction and posttranslational accumulation under drought, we first investigated whether the classical drought-hormone

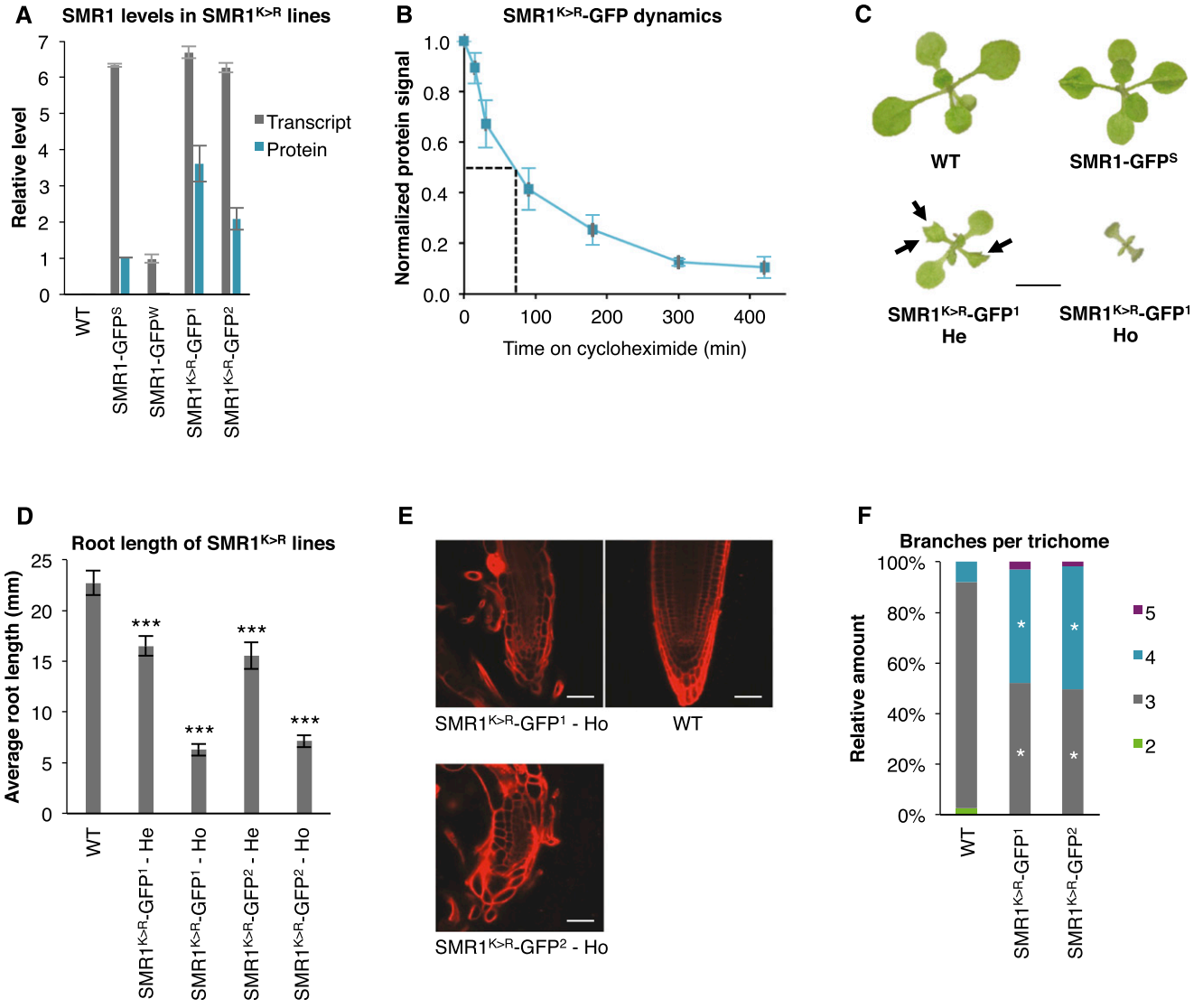

Figure 5. Molecular and phenotypic analysis of the Lys-less SMR1$^{K>R}$-GFP overexpression lines. A, SMR1 transcript (log_2 fold change) and protein levels in SMR1$^{K>R}$-GFP lines compared to the SMR1-GFP^{S} line with similar expression level. Values represent mean ± SE of 2 biological repeats. B, SMR1$^{K>R}$-GFP protein levels in the SMR1$^{K>R}$-GFP^{1} transgenic line over time upon treatment with 100 μM CHX. The intensity of the SMR1$^{K>R}$-GFP protein signal was normalized to the intensity of the loading control (Coomassie blue staining) and subsequently expressed relatively to the normalized signal at T0. The dotted line indicates the time at which the SMR1$^{K>R}$-GFP protein level was reduced by half (half-life). Mean ± SE, $n = 3$ biological repeats. C, Fifteen-day-old SMR1$^{K>R}$-GFP^{1} line grown in vitro. Representative seedlings are shown. Arrows point to leaf serrations. Scale bar = 5 mm. D, Root length measurements of SMR1$^{K>R}$-GFP overexpression lines at 12 DAS. Mean ± SE, $n = 4$ biological repeats, $^{***}P < 0.001$, ANOVA. E, Root tip of SMR1$^{K>R}$-GFP lines imaged after 9 d of growth in vitro. F, Trichome branching patterns in SMR1$^{K>R}$-GFP lines, measured on leaf 2 of 15-d-old seedlings. $n > 25$ trichomes per leaf, 8 plants per line, $^{*}P < 0.05$, Student's t test. In B and F, the SMR1$^{K>R}$-GFP plants were heterozygous.

ABA affects *SMR1* levels. Seedlings from the pSMR1::GUS line were grown under control conditions and transferred to ABA-containing growth medium at 9 d, for 24 h. In our experiments, no changes in GUS staining intensities or GUS pattern could be observed between ABA-treated and untreated seedlings, indicating that ABA does not transcriptionally induce *SMR1* (Fig. 7A; Supplemental Fig. S13). Using the same setup with the SMR1-GFP^{S} line, we also investigated whether ABA could trigger SMR1 protein accumulation, but it did not. More surprisingly, we even observed a clear and reproducible decrease in SMR1-GFP protein abundance after 4.5 and 24 h of treatment with ABA (Fig. 7, B and C; Supplemental Fig. S13). This decrease in SMR1 protein level could however be blocked by inhibiting the proteasome, indicating that ABA stimulates SMR1 protein turnover (Fig. 7B). From these data we conclude that, at least at the molecular

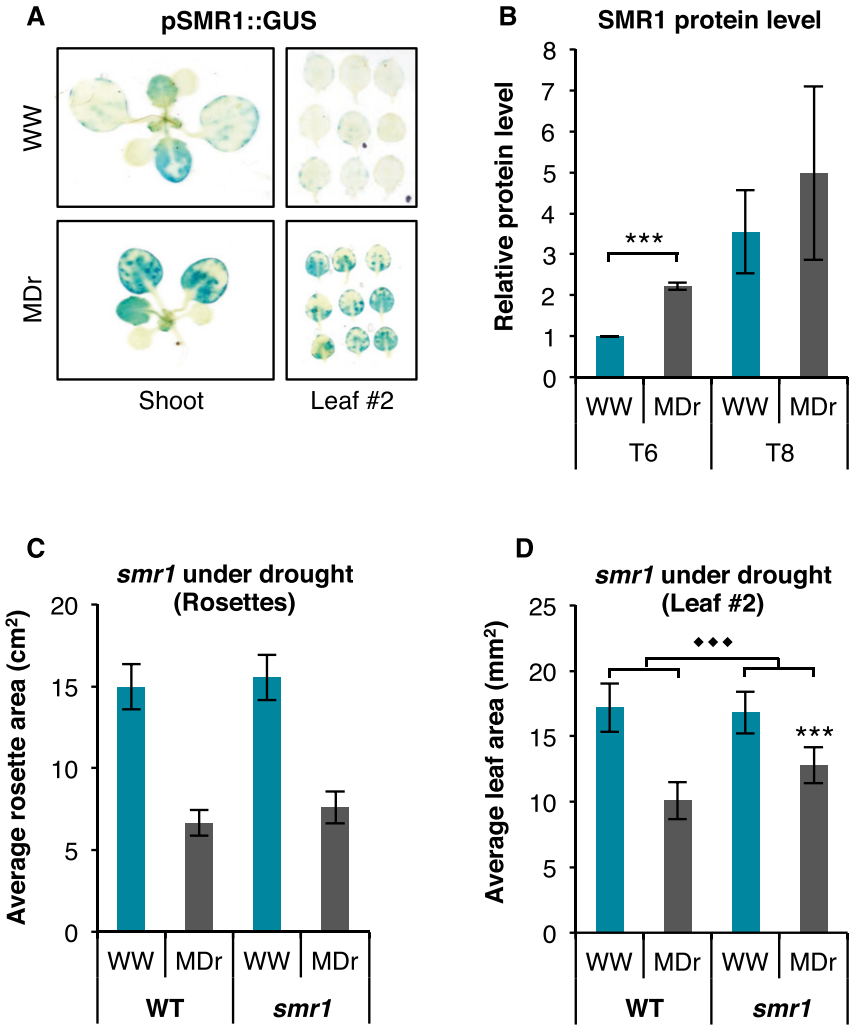

Figure 6. SMR1 expression, protein level, and mutant phenotype under moderate drought. A, SMR1 expression pattern in the pSMR1::GUS line subjected to well-watered (WW) or moderate drought (MDr) treatment (see "Materials and Methods"). B, SMR1-GFP protein levels in the SMR1-GFP^{S} line subjected to WW and MDr treatment during 6 (T6) or 8 (T8) days. Mean ± SE, $n = 3$ independent biological repeats, $^{***}P < 0.001$, Student's t test. C, Projected rosette area of full rosettes of *smr1* and wild-type controls subjected to long-term moderate drought conditions. Mean ± SE, $n = 2$ independent biological repeats, with 12 plants per line, per treatment, and per repeat. D, Area measurements of the second leaf of *smr1* mutants and wild-type controls subjected to a short-term moderate drought treatment of 8 d. Mean ± SE, $n = 6$ independent biological repeats, with >45 leaves per line, per treatment, per repeat. $^{***}P < 0.001$; ANOVA$_{TukeyHSD}$ compared to the wild type in the same condition. Three diamonds, $P < 0.001$, ANOVA-TREATMENT*GENOTYPE.

level, ABA does not mimic drought stress with regard to SMR1 regulation.

We subsequently tested whether other phytohormones, including ethylene (1-aminocyclopropane-1-carboxylic acid, ACC, the precursor of ethylene), auxin (1-Naphthaleneacetic acid, NAA), cytokinin (kinetin), jasmonate (methyl jasmonate), gibberellins (GA), and the GA antagonist paclobutrazol had the capacity to induce *SMR1* expression and protein accumulation. The defense hormone salicylic acid was not included in this analysis, but it was recently shown to negatively affect SMR1 levels (Hamdoun et al., 2016). As with ABA, we first exposed the pSMR1::GUS transgenic line to each of these hormones for 24 h and visualized GUS intensities and patterns in root tips (Fig. 7A; Supplemental Fig. S13A). In the mock treatment, GUS staining in pSMR1::GUS plants was only observed in the transition zone of the root tip. Interestingly, the area of GUS staining was enlarged in the presence of ACC and, to a lesser extent, cytokinin, resulting in pSMR1::GUS expression closer to the quiescent center (Fig. 7A; Supplemental Fig. S13). This suggests that these hormones stimulate pSMR1::GUS expression in the division zone or trigger a premature exit of cell division, thereby increasing the pSMR1::GUS expression closer to the root meristem.

We further explored whether these hormones could also affect SMR1-GFP protein levels (Fig. 7C). Among the tested hormones, only ACC could reproducibly increase SMR1-GFP protein levels at each measured time point (Fig. 7, C and D; Supplemental Fig. S13B). Similar to ABA, jasmonate and auxin had negative effects on SMR1-GFP protein levels, particularly at the later time points (Fig. 7C; Supplemental Fig. S13B). In conclusion, treatment of young seedlings with ACC had a positive effect on *SMR1* transcript levels and on SMR1 protein stability, which is similar to the effects observed under moderate drought stress. This similarity suggests that ethylene could be a candidate hormone acting upstream of SMR1 regulation under drought.

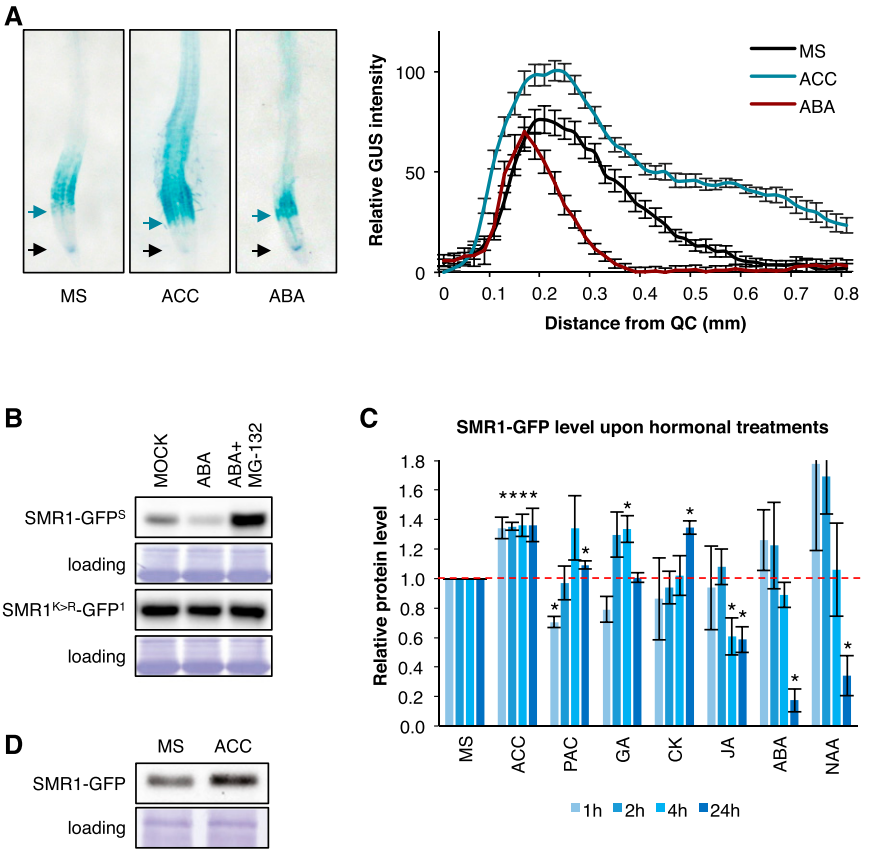

Figure 7. SMR1 expression and protein level following hormonal treatments. A, SMR1 expression pattern in pSMR1::GUS plants grown on MS and subsequently transferred to MS or MS supplemented with ABA or the ethylene precursor ACC for 24 h. Arrows point to quiescent centers (black) and the GUS-staining front (blue). The graph on the right shows the quantification of the GUS intensity along the first 0.8 mm of the roots, measured from the quiescent center in the proximal direction. The values represent the mean ± SD of $n = 12$ plants per treatment. B, SMR1-GFP protein levels in SMR1-GFP^S and SMR1$^{K>R}$-GFP^1 seedlings upon 50 μM ABA or ABA+MG-132 (proteasome inhibitor) treatment in liquid cultures for 4.5 h. C, SMR1-GFP protein levels in SMR1-GFP^S seedlings grown on MS and subsequently transferred to MS or MS supplemented with each phytohormone. The corresponding western blot is shown in Supplemental Figure S13B. Mean ± SE, $n = 3$ biological repeats. *$P < 0.05$; Student's t test compared to the level in MS (red dotted line) at the same time point. D, SMR1-GFP protein levels in SMR1-GFP^S seedlings exposed to 5 μM ACC for 1 h, as described in C. An extended version of this blot is shown in Supplemental Figure S13B.

DISCUSSION

Being exposed to variable environmental conditions, plants constantly reprogram their transcriptome and proteome to adapt to these conditions. Multiple abiotic and biotic stresses have been shown to induce a defense response and, in parallel, growth arrest of young developing organs (Claeys and Inzé, 2013; Yang and Li, 2017; Züst and Agrawal, 2017). In particular, drought stress is a very complex trait inducing specific responses depending on the organ and its developmental stage, as well as on the time of day and the severity of the drought treatment (Wilkins et al., 2010; Tardieu, 2012; Caldeira et al., 2014; Ma et al., 2014; Verslues, 2017). During the last decade, automated phenotyping with controlled watering has greatly contributed to our knowledge of physiological aspects of defense and growth arrest under drought. Several studies have demonstrated that growth inhibition and activation of defenses against stress are two distinct responses and that plants with improved tolerance to severe drought will not necessarily perform better in terms of growth when exposed to milder drought stress (Skirycz et al., 2011b; Tardieu, 2012). As a consequence, the experimental setup should be adequate for studying the growth response, with a particular focus on actively growing plant organs and a well-chosen timing at the moment of growth inhibition. At the molecular level, it has become clear that the growth reduction is not just a consequence of the activation of general tolerance mechanisms but that specific genes that are related to growth and induced by certain phytohormones are affected in actively growing plant organs (Baerenfaller et al., 2012; Avramova et al., 2015; Clauw et al., 2016; Dubois et al., 2017). Despite these efforts, the causal relation between altered transcriptome responses to drought and growth inhibition, particularly at the level of cell division arrest, largely remain unclear. In this study, we have provided experimental evidence that supports a role for SMR1 as one of the possible inhibitors of the cell cycle and growth under drought.

SMR1-Mediated Cell Cycle Inhibition Might Be Effective in Restricting Growth under Drought

Previous work showed that when growing leaves are exposed to drought stress, cell division arrest is the main contributor to leaf growth reduction (Avramova et al., 2015). However, molecular links between drought and its effects on the cell cycle have only begun to emerge. For instance, Arabidopsis plants deficient in CYCLIN-DEPENDENT KINASE C;2 (CDKC;2), a negative regulator of cell division, show enhanced tolerance to drought stress (Zhao et al., 2017). In maize (*Zea mays*), a search for cell cycle inhibitory genes

induced by drought stress pointed toward orthologs of the CDK-activating phosphatase CDC25, and KRP2, but the downstream molecular mechanisms were not investigated further (Avramova et al., 2015). In our study, none of the KRP family genes were responsive to drought. In contrast, a pronounced transcriptional response was observed for members of the SMR gene family, supporting the idea that SMRs are more responsive to external signals (Peres et al., 2007), while KRPs are more involved in endogenous development.

Our study focuses on *SMR1* since this CKI shows a rapid and clear transcriptional induction in young leaves exposed to moderate drought. This observation is in accordance with a study in rice (*Oryza sativa*), in which an ortholog of *SMR1*, *EL2* (Os3g01740), was also quickly induced by drought (Peres et al., 2007). Nevertheless, as correctly pointed out by Baerenfaller et al. (2012), drought responses at the transcriptome level do not necessarily reflect changes at the protein level. In the case of *SMR1*, both transcript and protein levels increased under drought. Besides *SMR1*, several other CKIs, such as *SIM*, *SMR8*, and *SMR10*, were also responsive to drought stress, but later during leaf development, when leaf growth is mainly driven by cell expansion. In contrast, the expression of *SMR5* showed both early induction and a gradual increase in transcript levels during leaf development under drought, reaching its maximum in full-grown leaves. Notably, *SMR5* has previously been shown to be responsive to ROS and involved in DNA repair (Yi et al., 2014). It is likely that in our experiment, the prolonged drought, as perceived by the older leaves, triggers the accumulation of ROS, which could explain the induction of *SMR5*. Although the function of this gene has not been investigated in this study, we do not exclude its involvement in cell division inhibition under drought and this may deserve further investigation.

At the molecular level, we speculate that SMR1 protein accumulation under drought stress might contribute to cell division inhibition, possibly by binding to CDKs. In particular, the SMR1 interaction with CDKB1 complexes might inhibit its kinase activity, which is required to enter mitosis, in a way similar to the inhibitory action of KRPs on CDKBs that also block mitosis when overexpressed (Verkest et al., 2005; Weinl et al., 2005). This assumption is supported by the interaction between SMR1 and CDKB1, the flow cytometry data pointing toward M-phase inhibition, and the decrease in growth and cell division of SMR1-overexpressing plants. Such a scenario is also in line with our phenotypic data, which show that plants lacking *SMR1* show a slightly less pronounced short-term growth inhibition under drought as compared to wild-type plants. This growth advantage is nevertheless not sustained when the stress holds for longer, most likely because of a decrease in cell expansion that is actively controlled by the plant and regulates the growth at organ level in order to limit unnecessary evaporation and avoid detrimental consequences of maintaining growth under drought. Importantly, it is clear that the proposed model for SMR1 is a simplification of the complex growth-inhibitory pathway and that additional factors are certainly also involved in this process, which could explain the considerable growth reduction (24%) observed in *smr1* mutants exposed to drought (Fig. 6D).

Ethylene Signaling Upstream of SMR1 in the Drought Response

A large majority of plant responses to drought are attributed to the phytohormone ABA, which is responsible for stomatal closure as well as the accumulation of compounds and proteins protecting the plant from dehydration mainly in mature tissues (Seki et al., 2007). Our study, however, does not provide evidence that ABA induces *SMR1* transcription. Instead, the *SMR1* expression appeared to be slightly decreased when seedlings are exposed to ABA. Similar observations were made in rice, where the *SMR1* homolog *EL2* (Os03g01740) is transcriptionally induced by drought, but through an ABA-independent pathway (Peres et al., 2007). Even more intriguing is the finding that ABA triggers proteasome-mediated degradation of SMR1, making the involvement of ABA in the cell division arrest in young leaves exposed to drought stress unlikely. Notably, previous work already revealed that the transcript levels of ABA-related genes did not vary along with the dynamics of growth inhibition of young leaves (Dubois et al., 2017). Moreover, in a large-scale expression analysis performed on proliferative leaf tissue, a set of differentially expressed genes enriched for ABA-related genes is common to a broad range of Arabidopsis accessions regardless of whether they block growth under drought or instead show less growth inhibition (Clauw et al., 2016).

Based on our data, we propose that the growth-inhibitory hormone ethylene acts upstream of *SMR1* induction. Ethylene is already known to inhibit plant growth and several connections between ethylene signaling and cell cycle inhibition exist. For instance, ethylene inhibits cell proliferation of the Arabidopsis root meristem (Thomann et al., 2009; Street et al., 2015). Also, in young proliferating Arabidopsis leaves subjected to osmotic stress, ethylene negatively balances cell cycle progression via inhibition of CDKA activity (Skirycz et al., 2011b). In poplar (*Populus* spp.), ethylene-induced dwarfism has also been proposed to result in the down-regulation of multiple cell cycle genes, including *CYCLINs* (Plett et al., 2014). Interestingly, more recent studies performed in the field have proven the involvement of ethylene in regulating maize growth under drought (Habben et al., 2014; Shi et al., 2017). Together, these studies demonstrated that mutations in the genes involved in ethylene biosynthesis and response affect growth of different plant species under drought stress (Beltrano et al., 1999; Habben et al., 2014; Shi et al., 2015; Dubois et al., 2017). However, the precise molecular pathway connecting

ethylene to cell cycle inhibition under drought remained unclear. Based on our data, we propose that ethylene induces *SMR1* expression and protein accumulation under drought. We speculate that *SMR1* is a direct target of EIN3, the central primary transcription factor downstream of the ethylene-signaling pathway, since its promoter contains an EIN3-binding site (ATGTAT) 136 bp upstream of the start codon (Song et al., 2015). The subsequent accumulation of SMR1 protein is most likely a result of the decreased CDKA activity observed in young leaves of plants exposed to ethylene (Skirycz et al., 2011a). In our hypothetical model, reduced CDKA activity would reduce SMR1 phosphorylation, which may at least in part stabilize the protein.

Proteasome-Mediated Degradation of SMR1 Is Crucial to Enable Plant Growth

Plant growth is controlled by at least six cellular mechanisms, including cell division rate and duration (Gonzalez et al., 2012). As illustrated by the higher-order *krp* mutants and the *smr2* mutant with larger shoots (Cheng et al., 2013; Kumar et al., 2015), CKI proteins restrict cell proliferation during leaf growth even under nonstress conditions. *SMR1* is also expressed under nonstress conditions and participates in the regulation of leaf and root growth, since *smr1* mutants show a slight increase in leaf area and root length, which is most pronounced at the cellular level. Although plants overexpressing *SMR1* at a moderate level had no drastic growth phenotypes, overexpression of nondegradable *SMR1* severely affected plant growth, in both the shoot and roots. These phenotypes are similar to those of seedlings overexpressing other CKIs such as *SIM* or *KRP1*, *-2*, *-3*, or *-6* (Wang et al., 2000; De Veylder et al., 2001; Weinl et al., 2005; Churchman et al., 2006; Liu et al., 2008; Jun et al., 2013; Noir et al., 2015). An even stronger growth inhibitory phenotype is observed when plants express a more stable form of SMR1. This also entails that under growth-favorable conditions, active degradation of SMR1 is absolutely crucial to allow plant growth.

In plants and animals, a widespread mechanism for protein degradation is the ubiquitin 26S-proteasome system (UPS; Ciechanover et al., 2000; Vierstra, 2009). Many proteins targeted by this pathway are recognized by F-box proteins, often upon phosphorylation, which trigger their ubiquitylation and subsequent degradation. In metazoans, the CKI protein $p27^{KIP1}$ becomes unstable when cells enter S-phase and its degradation requires phosphorylation by the CYCE/CDK2 complex in order to be recognized by SCF^{SKP2} (SKP2 being a LRR-type F-box protein; Starostina and Kipreos, 2012). This phosphorylation causes CKI protein degradation in the nucleus, while degradation that is independent of its phosphorylation occurs in the cytosol (Kamura et al., 2004). While our experiments have provided evidence that SMR1 is degraded via the UPS, the molecular players involved in its phosphorylation and subsequent recognition by a CRL-type E3 ubiquitin-ligase still remain to be elucidated. We believe that CDKA is a good candidate for phosphorylating SMR1 prior to its degradation since SMR1 and CDKA interact, and so does the most unstable C-terminal part of the protein. Moreover, mutation of the TPIK site rendered the SMR1 protein slightly more stable, though this phosphorylation site is located at the N terminus, the most stable half of SMR1. This suggests that additional motif(s) necessary for SMR1 degradation are also present in the C-terminal part of the protein. Finally, based on the resemblance in phenotype between the mutant of *FBL17* (the F-box targeting KRP2 protein for degradation; Noir et al., 2015) and the SMR1-stabilizing plants, we speculated that FBL17 would be a suitable candidate F-box protein to target SMR1 for degradation, but this was not the case. Another candidate CRL-type E3 ubiquitin-ligase is SCF^{SKP2b}, which is involved in KRP1 degradation (Ren et al., 2008). However, the lack of an impaired leaf growth phenotype in SKP2b RNAi lines raises doubts about its involvement in SMR1 degradation. Thus, it will be compelling to identify the E3 ubiquitin ligase involved in SMR1 protein decay and to study its activity under drought and other stress conditions.

CONCLUSION

We studied the molecular mechanisms and physiological importance of posttranslational control of SMR1. Our results suggest that CDKA may be involved in the regulation of SMR1 stability, and we speculate that CDKA might phosphorylate SMR1 prior to degradation. Subsequently, SMR1 is recognized by a yet unknown CRL-type E3 ligase complex, targeting SMR1 for ubiquitin-mediated proteasomal degradation. Degradation of SMR1 is absolutely crucial to enabling plant growth, since accumulation of more stable SMR1 proteins causes severe dwarfism. Thus, under growth-favorable environmental conditions, SMR1 turnover is fast, while under unfavorable conditions, the SMR1 protein is stabilized to block cell cycle progression. Here, we observed a quick transcriptional induction and protein accumulation of SMR1 under moderate drought stress conditions. We propose that ethylene may act upstream of SMR1. Ethylene and osmotic stress are known to reduce the activity of the CDKA protein, which could decrease SMR1 protein decay. As a result, the SMR1 protein is more abundant and may act as a negative regulator of cell division of leaves and roots, possibly through the inhibition of CDKB1, and by pushing dividing cells toward differentiation.

MATERIALS AND METHODS

Plant Material

The *smr1* mutant (SALK_033905), previously described by Kumar et al. (2015), was a kind gift from Prof. John Larkin (LA State University). The making

of the *fbl17-1* (GABI-170E02) mutant was described previously (Gusti et al., 2009). The pSMR1::GUS line, previously described by Yi et al. (2014), was a kind gift from Prof. Lieven De Veylder (VIB Ghent, Belgium). The pSMR1::SMR1-GFP and 35S::SMR$^{K>R}$-GFP lines were generated by Gateway cloning using the pK7m34GW and pB7FWG2 vectors, respectively (Supplemental Table S2). The SMR$^{K>R}$ Lys-less sequence was obtained by DNA synthesis. All lines are homozygous, with the exception of the 35S::SMR1$^{K>R}$-GFP lines that are the segregating T2, and the *fbl17-1* × SMR1-GFP cross that is the segregating F2. All lines are in a Col-0 background and were upscaled and grown with the corresponding Col-0 wild type.

In Soil Plant Growth Conditions on the PHENOPSIS Platform

Seeds were kept in the dark at 4°C before sowing. Four to six seeds were sown per pot filled with a 1:1 (v:v) mixture of loamy soil and organic compost (Neuhaus N2, 0.75 g_{H20}/g_{soil}). The pots were placed in the PHENOPSIS growth chamber and kept in darkness for 48 h (20°C, 68% air relative humidity). Afterward, they received a daily cycle of 12 h light, 175 μmol m^{-2} s^{-1} photosynthetic photon flux density, 0.75 kPa water vapor pressure deficit and air temperature set to 20°C. Pots were sprayed with water three times per day until the sixth true leaf emerged from the shoot apical meristem. Then, soil water content was automatically adjusted individually in every pot by daily watering: soil water content was maintained at 0.35 g_{H20}/g_{soil} for half of the pots (well-watered treatment corresponding to 45% of the field water capacity [FWC]) and watering was withheld for the other half of the pots until a soil water content of 0.22g_{H20}/g_{soil} was reached (moderate water deficit treatment corresponding to 28% of the FWC). During the first experiment (Fig. 1), samples of the sixth leaf of Col-0 plants were harvested at different developmental stages, ranging from young leaves in the proliferation stage to mature leaf tissue, and expression analysis was performed to measure the transcript levels of all genes from the *KRP* and *SMR* gene families. During two other experiments (Fig. 2D), Col-0 and *smr1* were grown together for leaf measurements and cellular analyses on leaves 6 and 22.

In Vitro Plant Growth Conditions

For in vitro cultures, Arabidopsis (*Arabidopsis thaliana*) seeds were surface-sterilized with 70% ethanol and 0.05% Tween 20 for 10 min, followed by two washes with 96% ethanol. Sterile seeds were sown on 0.5× Murashige and Skoog (MS) medium supplemented with 1% Suc (Sigma-Aldrich). For the experiments involving treatments with chemicals or phytohormones (Figs. 3, A and B, 4, A and B, 5B, and 7), 0.68% agar (Sigma-Aldrich) was added to the medium, and the medium was overlaid with a nylon mesh (40 μm; Sefar Fyltis) prior to sowing. Agar (1.2%) was added for the experiments requiring growth in the vertical orientation for root analysis (Figs. 1, A, C, E, and F, and 5, D and E), and 0.8% agar was used for all other experiments, requiring growth on horizontal petri dishes without nylon mesh. A stratification period of 48 h was included. All plants were grown in a 16-h-light (21°C) and 8-h-dark (18°C) regime.

For the experiments involving treatments with CHX, MG-132, or MLN on Arabidopsis lines (Fig. 4, A and B, 5B, and 7B), 8-d-old seedlings were transferred from the petri dishes to liquid medium containing either 100 μM CHX (Sigma-Aldrich), 100 μM MG-132 (Sigma-Aldrich), 25 μM MLN4924 (Active Biochem), 50 μM ABA (Sigma-Aldrich; for Fig. 7B), or mock (water). Vacuum infiltration was performed for two times for 5 min at 500 mmHg. Upon infiltration, the seedlings were placed back in the growth room.

For the hormone treatments (Fig. 7, A, C, and D), 8-d-old seedlings were transferred to a fresh petri dish with 0.5× MS medium supplemented with hormones, by transferring the mesh in sterile conditions from one plate to the other. The new medium (0.68% agar) was supplemented with either 5 μM ACC (Sigma-Aldrich), 1 μM paclobutrazol (Duchefa), 10 μM GA (Duschefa), 0.5 μM kinetin (Serva), 10 μM methyl jasmonate (Duschefa), 50 μM ABA (Sigma-Aldrich), or 0.5 μM NAA (Duschefa). Upon transfer, the plates were placed back in the growth room.

In Soil Plant Growth Conditions with Manual Watering

The seeds were stratified in water and darkness for 48 h. For growth measurements under control conditions (as in Fig. 2B), plastic pots (7 × 7 × 7 cm) were filled with 62 g of soil (Hawita Standard-T, 50% relative water content [RWC], 4.6 g_{H20}/g_{soil} FWC) and watered with 35 mL of tap water to reach a relative humidity of 2.2 g_{H20}/g_{soil} (RWC 69%). Three seeds were sown in the middle of the pot. The pots were covered with a plastic foil to maintain the humidity level and placed in a 16-h-light (21°C) and 8-h-dark (18°C) regime. At 4 DAS, the plastic film was removed, and at 5 DAS plants were thinned out to keep one plant per pot. The pots were watered every 2 to 3 d and maintained at a relative soil humidity of 2.2 g_{H20}/g_{soil}.

For the experiments requiring drought stress treatments as described in Figure 6, seeds and pots were prepared as described above, but pots were watered to a soil relative humidity level of 1.7 g_{H20}/g_{soil} (RWC 63%). This reduced RWC enabled proper seed germination while ensuring that the drought-stressed pots reached moderate drought levels quickly upon water withholding. Per pot, 4× three seedlings were grown until 5 DAS as described above, and seedlings were thinned out to keep four plants per pot. At 6 DAS, the drought treatment started (T1). Half of the pots were watered until 2.2 g_{H20}/g_{soil} for well-watered controls. These pots were weighted and watered daily to keep the soil relative humidity at 2.2 g_{H20}/g_{soil}. The other half of the pots were left to dry out, weighed daily, and reached the moderate drought level (1.2 g_{H20}/g_{soil} or RWC 55%) at T7. Leaf samples for expression and protein level analysis were harvested at T6 and T8. Leaf samples for leaf area measurements were harvested at T8 for the short-term drought (Fig. 6D) and at 22 DAS for the long-term drought (Fig. 6C).

Leaf Measurements and Cellular Analysis

For the detailed rosette area measurements that are shown in Figure 2B, plant size at 22 DAS was determined by dissecting every leaf and placing it from oldest to youngest on a petri dish with 1% agar. For Figure 6C, the rosettes were directly placed on a petri dish with agar without dissecting the leaves. The plates were photographed and the rosette and leaf areas were measured with ImageJ v1.45 (NIH; https://rsb.info.nih.gov/ij/). Three biological replicates were performed with 10 plants per line, per replicate, and per treatment.

For measurements of the second leaf, as shown in Figure 6D, the second leaf of each plant was harvested at T8 (13 DAS), placed on a petri dish with 1% agar, photographed, and measured in ImageJ v1.45. Six biological replicates were performed with at least 45 plants per line, per treatment, and per replicate.

For cellular analysis of leaf 6 and leaf 22 (Fig. 2D; Supplemental Fig. S3), the leaves were harvested 2 and 4 d after their respective emergence (length between 1.5 and 2.5 mm) and at maturity. Three to four leaves per date per genotype were considered, except for the data shown in Figure 2D, where 12 leaves were considered. As soon as the leaf was harvested, it was placed on a sheet of paper and scanned, and its area was defined in ImageJ. A negative imprint of the adaxial epidermis was obtained after evaporation of a varnish spread on its surface. These epidermal imprints were analyzed using a microscope (Leitz DM RB; Leica) supported with ImageJ v1.48 (NIH; https://rsb.info.nih.gov/ij/). Mean epidermal cell densities (cells mm^{-2}) were estimated by counting the number of epidermal cells in four zones on each leaf. Total epidermal cell numbers in each leaf were estimated from epidermal cell density and leaf area. Mean epidermal cell area (μm^2) was calculated as the reciprocal of epidermal cell density.

Root Length Analysis and Confocal Imaging

After 12 d of growth in vitro in the vertical orientation, the plates were scanned and the root length was measured with ImageJ. For root meristem measurements (Fig. 2C) and the imaging of the root tip (Figs. 2F and 5E), the roots were mounted on a microscopic slide in a 75 μg/mL propidium iodide solution. Root tips were imaged under the confocal microscope (Leica TCS SP8) in the plane of the quiescent center. The meristem size was measured in ImageJ as the distance between the quiescent center and the last dividing cell of the cortex (see Supplemental Fig. S2).

Expression of (Parts of) SMR1-GFP and CDKA-RFP in *Nicotiana benthamiana* Leaves

For protein expression in *N. benthamiana* leaves (Figs. 3E and 4C), *Agrobacterium tumefaciens* GV3101 cultures containing the construct of interest (full-length SMR1 fused to GFP, or parts of SMR1 fused to GFP, and CDKA;1 fused to RFP; Supplemental Table S2) were grown for 24 h in liquid cultures. A culture with the silencing suppressor p19 was included. The pelleted bacteria were subsequently diluted and mixed with the p19 strain, each to an $OD_{0.3}$ in a 10 mM $MgCl_2$ solution. Young leaves of 3-week-old plants were infiltrated with the

mixtures in such a way that the different constructs were always infiltrated side-by-side on the same leaf to avoid differences in expression. The plants were placed back in the growth room for 72 h. Subsequently, half of the leaves were infiltrated directly with a 100 μM CHX (Sigma-Aldrich) solution and the other half with the mock solution. At least three leaves per construct per treatment were infiltrated. Nine patches of equal size were harvested from each infiltrated spot per construct, per treatment. The whole experiment was repeated twice.

GUS Staining

For GUS expression analysis in the pSMR1::GUS line, seedlings were first incubated in 80% acetone for 20 min. The acetone was washed away with GUS buffer (50 mM Na_2PO_4, pH7.2, 2 mM $K_4[Fe(CN)_6]$*$3H_2O$, 2 mM $K_3[Fe(CN)_6]$, and 0.2% Triton) and replaced by a 2 mM X-Gluc (Euromedex) solution in GUS buffer. The staining was performed by a 3-h incubation at 37°C. The seedlings were washed in ethanol, destained overnight in 96% ethanol, and mounted on microscope slides in lactic acid.

Expression Analysis by RT-qPCR

For expression analysis by RT-qPCR, individual leaves (Fig. 1, Leaf #6 at growth stages L6-1, L6-2, L6-3, L6-4, L6-5, and L6-6, with 6 to 10 leaves per sample) or whole 7-d-old seedlings (Fig. 5A; Supplemental Fig. S9C) were collected. Plant tissue was flash-frozen in liquid nitrogen and ground with the Silamat S6 (Ivoclar Vivadent). Total RNA was extracted with the Nucleospin RNA XS kit (Macherey Nagel; Fig. 1) or with Trizol (Invitrogen) followed by precipitation with isopropanol and a wash with 70% ethanol (Fig. 5A; Supplemental Fig. S9C). For each sample, cDNA was synthesized from 1 μg of RNA. RT-qPCR was performed with the LightCycler480 (Bio-Rad) using the primers listed in Supplemental Table S1, and the data were analyzed as previously reported (Dubois et al., 2017). In brief, three technical replicates were performed, their cycle threshold values (Ct-value) were averaged, and differences in unequal cDNA amounts were corrected for by normalizing to two housekeeping genes (*EXP*, *AT4G26410*; *TIP4.1*, *AT4G34270*). The fold change was calculated by comparing the normalized Ct values between both conditions (drought versus well-watered; Fig. 1) or between the different genotypes (transgenic lines versus the wild type; Fig. 5A; Supplemental Fig. S9C). For each experiment, two independent biological replicates were performed, and both experiments had similar results. The presented data show one biological replicate.

Protein Analysis and Western Blotting

Arabidopsis seedlings or *N. benthamiana* leaf patches were flash-frozen in liquid nitrogen and ground with the Silamat S6 (Ivoclar Vivadent). Protein extraction and western blotting were performed as described previously (Derrien et al., 2012) with Bio-Rad 4 to 15% precast gradient gels. The SMR1-GFP protein was detected with the anti-GFP JL8 antibody (Clontech), CDKA with the anti-PSTAIRE antibody (Santa Cruz Biotechnology), and CDKB with an anti-CDKB1 antibody (described in Verkest et al., 2005) kindly provided by Lieven de Veylder (VIB Ghent, Belgium). Antibodies were diluted at 1:2,000, 1:10,000, and 1:2,000, respectively, in 5% milk in TBS-T.

Immunoprecipitation

Plant tissues were homogenized and the powder was resuspended in ice-cold protein extraction buffer (10 mM Tris-HCl, pH 7.5, 150 mM NaCl, 0.5 mM EDTA, 0.5% Nonidet P-40, and 1× protease inhibitor tablet [Roche]) for 1 h at 4°C on a rotating wheel. The insoluble fraction was removed by centrifugation and the supernatant was incubated with 30 μL of anti-GFP-coated magnetic beads (GFP-Trap_M; Chromotek) for 2 h and further treated according to the manufacturer's instructions. Proteins were eluted in denaturing 1× Laemmli buffer (95°C) with 50 mM DTT. Bead-bound proteins were visualized by western blotting as described above.

FLIM-FRET Analysis

N. benthamiana leaves were infiltrated with various constructs (GFP-fusion as donor, RFP-fusion as acceptor, and p19) as described above. Plants were placed back in the growth room for 48 h, and the expression of both constructs in each infiltrated leaf was carefully viewed with the confocal microscope. When >80% of the cells showed coexpression, FLIM-FRET was performed with the Nikon Eclipse TE 2000-U microscope. The fluorescence decay rate of GFP(fusion) was measured with the LIFA frequency domain fluorescence lifetime imaging system (Lambert Instruments) in 50 nuclei per sample, per biological replicate. The GFP half-life in nuclei of the interaction samples (SMR1-GFP/CDKA-RFP and SMR1-GFP/BPM6-RFP) was compared to the GFP half-life in nuclei of control samples, in which only SMR1-GFP was transformed. The donor-FRET efficiency was estimated as %FRET = 1-(t(donor-acceptor)/t(donor)).

Flow Cytometry

The second leaves of >12 plants per line were harvested and flow cytometry was performed as described previously (Noir et al., 2015). At least two biological replicates were performed.

Accession Numbers

The accession numbers of the main genes mentioned in this study are as follows: AT5G04470 (*SIM*), AT3G10525 (*SMR1/LGO*), AT1G08180 (*SMR2*), AT5G02420 (*SMR3*), AT5G02220 (*SMR4*), AT1G07500 (*SMR5*), AT5G40460 (*SMR6*), AT3G27630 (*SMR7*), AT1G10690 (*SMR8*), AT1G51355 (*SMR9*), AT2G28870 (*SMR10*), AT2G28330 (*SMR11*), AT2G37610 (*SMR12*), AT3G20898 (*SMR13*), AT2G23430 (*KRP1*), AT3G50630 (*KRP2*), AT5G48820 (*KRP3*), AT2G32710 (*KRP4*), AT3G24810 (*KRP5*), AT3G19150 (*KRP6*), AT1G49620 (*KRP7*), and AT3G48750 (*CDKA;1/CDC2*),

Supplemental Data

The following supplemental materials are available.

Supplemental Figure S1. Rosette size measurements of *smr1* mutants compared to the wild type.

Supplemental Figure S2. Root meristems of *smr1* mutants compared to the wild type.

Supplemental Figure S3. Cellular analysis of *smr1* epidermal leaf cells during leaf development.

Supplemental Figure S4. Complementation of the cellular defects of the *smr1* mutant by introgression of the SMR1-GFP^{W} construct.

Supplemental Figure S5. Expression pattern of pSMR1::SMR1-GFP.

Supplemental Figure S6. Rosette area measurements of SMR1-GFP^{S} seedlings compared to the wild type.

Supplemental Figure S7. Cellular localization of the SMR1-GFP and CDKA-RFP proteins used for FLIM-FRET.

Supplemental Figure S8. Presence of a putative CDKA phosphorylation site and conserved motifs in SMR family genes.

Supplemental Figure S9. SMR1-GFP protein dynamics and protein stability in the *fbl17* mutant.

Supplemental Figure S10. Characterization of truncated variants of SMR1.

Supplemental Figure S11. SMR1$^{K>R}$-GFP level upon 4 h treatment with cycloheximide alone or in combination with MG-132 or MLN4924.

Supplemental Figure S12. Trichome branching and leaf ploidy level in the SMR1$^{K>R}$-GFP overexpression line.

Supplemental Figure S13. *SMR1* expression and protein level upon hormonal treatments.

Supplemental Table S1. Primers used for RT-qPCR.

Supplemental Table S2. Primers used for cloning SMR1 (parts) and CDKA.

ACKNOWLEDGMENTS

We thank our team for assistance and scientific input and Dr. Lieven De Veylder and Prof. John Larkin for sharing seeds and for fruitful discussions.

Received November 30, 2017; accepted February 10, 2018; published February 22, 2018.

LITERATURE CITED

Araus JL, Slafer GA, Reynolds MP, Royo C (2002) Plant breeding and drought in C3 cereals: what should we breed for? Ann Bot **89:** 925–940

Avramova V, AbdElgawad H, Zhang Z, Fotschki B, Casadevall R, Vergauwen L, Knapen D, Taleisnik E, Guisez Y, Asard H, Beemster GT (2015) Drought induces distinct growth response, protection, and recovery mechanisms in the maize leaf growth zone. Plant Physiol **169:** 1382–1396

Baerenfaller K, Massonnet C, Walsh S, Baginsky S, Bühlmann P, Hennig L, Hirsch-Hoffmann M, Howell KA, Kahlau S, Radziejwoski A, et al (2012) Systems-based analysis of Arabidopsis leaf growth reveals adaptation to water deficit. Mol Syst Biol **8:** 606

Beltrano J, Ronco MG, Montaldi ER (1999) Drought stress syndrome in wheat is provoked by ethylene evolution imbalance and reversed by rewatering, aminoethoxyvinylglycine, or sodium benzoate. J Plant Growth Regul **18:** 59–64

Bonhomme L, Valot B, Tardieu F, Zivy M (2012) Phosphoproteome dynamics upon changes in plant water status reveal early events associated with rapid growth adjustment in maize leaves. Mol Cell Proteomics **11:** 957–972

Boniotti MB, Gutierrez C (2001) A cell-cycle-regulated kinase activity phosphorylates plant retinoblastoma protein and contains, in Arabidopsis, a CDKA/cyclin D complex. Plant J **28:** 341–350

Caldeira CF, Jeanguenin L, Chaumont F, Tardieu F (2014) Circadian rhythms of hydraulic conductance and growth are enhanced by drought and improve plant performance. Nat Commun **5:** 5365

Cheng Y, Cao L, Wang S, Li Y, Shi X, Liu H, Li L, Zhang Z, Fowke LC, Wang H, Zhou Y (2013) Downregulation of multiple CDK inhibitor ICK/KRP genes upregulates the E2F pathway and increases cell proliferation, and organ and seed sizes in Arabidopsis. Plant J **75:** 642–655

Churchman ML, Brown ML, Kato N, Kirik V, Hülskamp M, Inzé D, De Veylder L, Walker JD, Zheng Z, Oppenheimer DG, et al (2006) SIAMESE, a plant-specific cell cycle regulator, controls endoreplication onset in *Arabidopsis thaliana*. Plant Cell **18:** 3145–3157

Ciechanover A, Orian A, Schwartz AL (2000) Ubiquitin-mediated proteolysis: biological regulation via destruction. BioEssays **22:** 442–451

Claeys H, Inzé D (2013) The agony of choice: how plants balance growth and survival under water-limiting conditions. Plant Physiol **162:** 1768–1779

Clauw P, Coppens F, Korte A, Herman D, Slabbinck B, Dhondt S, Van Daele T, De Milde L, Vermeersch M, Maleux K, et al (2016) Leaf growth response to mild drought: natural variation in Arabidopsis sheds light on trait architecture. Plant Cell **28:** 2417–2434

Coelho CM, Dante RA, Sabelli PA, Sun Y, Dilkes BP, Gordon-Kamm WJ, Larkins BA (2005) Cyclin-dependent kinase inhibitors in maize endosperm and their potential role in endoreduplication. Plant Physiol **138:** 2323–2336

De Veylder L, Beeckman T, Beemster GT, Krols L, Terras F, Landrieu I, van der Schueren E, Maes S, Naudts M, Inzé D (2001) Functional analysis of cyclin-dependent kinase inhibitors of Arabidopsis. Plant Cell **13:** 1653–1668

De Veylder L, Beeckman T, Inzé D (2007) The ins and outs of the plant cell cycle. Nat Rev Mol Cell Biol **8:** 655–665

De Veylder L, Segers G, Glab N, Casteels P, Van Montagu M, Inzé D (1997) The Arabidopsis Cks1At protein binds the cyclin-dependent kinases Cdc2aAt and Cdc2bAt. FEBS Lett **412:** 446–452

Derrien B, Baumberger N, Schepetilnikov M, Viotti C, De Cillia J, Ziegler-Graff V, Isono E, Schumacher K, Genschik P (2012) Degradation of the antiviral component ARGONAUTE1 by the autophagy pathway. Proc Natl Acad Sci USA **109:** 15942–15946

Dissmeyer N, Schnittger A (2011) Use of phospho-site substitutions to analyze the biological relevance of phosphorylation events in regulatory networks. Methods Mol Biol **779:** 93–138

Dubois M, Claeys H, Van den Broeck L, Inzé D (2017) Time of day determines Arabidopsis transcriptome and growth dynamics under mild drought. Plant Cell Environ **40:** 180–189

Genschik P, Marrocco K, Bach L, Noir S, Criqui MC (2014) Selective protein degradation: a rheostat to modulate cell-cycle phase transitions. J Exp Bot **65:** 2603–2615

Gonzalez N, Vanhaeren H, Inzé D (2012) Leaf size control: complex coordination of cell division and expansion. Trends Plant Sci **17:** 332–340

Granier C, Aguirrezabal L, Chenu K, Cookson SJ, Dauzat M, Hamard P, Thioux JJ, Rolland G, Bouchier-Combaud S, Lebaudy A, et al (2006) PHENOPSIS, an automated platform for reproducible phenotyping of plant responses to soil water deficit in Arabidopsis thaliana permitted the identification of an accession with low sensitivity to soil water deficit. New Phytol **169:** 623–635

Gusti A, Baumberger N, Nowack M, Pusch S, Eisler H, Potuschak T, De Veylder L, Schnittger A, Genschik P (2009) The Arabidopsis thaliana F-box protein FBL17 is essential for progression through the second mitosis during pollen development. PLoS One **4:** e4780

Gutierrez C (2005) Coupling cell proliferation and development in plants. Nat Cell Biol **7:** 535–541

Habben JE, Bao X, Bate NJ, DeBruin JL, Dolan D, Hasegawa D, Helentjaris TG, Lafitte RH, Lovan N, Mo H, Reimann K, Schussler JR (2014) Transgenic alteration of ethylene biosynthesis increases grain yield in maize under field drought-stress conditions. Plant Biotechnol J **12:** 685–693

Hamdoun S, Zhang C, Gill M, Kumar N, Churchman M, Larkin JC, Kwon A, Lu H (2016) Differential roles of two homologous cyclin-dependent kinase inhibitor genes in regulating cell cycle and innate immunity in Arabidopsis. Plant Physiol **170:** 515–527

Harashima H, Dissmeyer N, Schnittger A (2013) Cell cycle control across the eukaryotic kingdom. Trends Cell Biol **23:** 345–356

Harb A, Krishnan A, Ambavaram MM, Pereira A (2010) Molecular and physiological analysis of drought stress in Arabidopsis reveals early responses leading to acclimation in plant growth. Plant Physiol **154:** 1254–1271

Inagaki S, Umeda M (2011) Cell-cycle control and plant development. Int Rev Cell Mol Biol **291:** 227–261

Jakoby MJ, Weinl C, Pusch S, Kuijt SJ, Merkle T, Dissmeyer N, Schnittger A (2006) Analysis of the subcellular localization, function, and proteolytic control of the Arabidopsis cyclin-dependent kinase inhibitor ICK1/KRP1. Plant Physiol **141:** 1293–1305

Jun SE, Okushima Y, Nam J, Umeda M, Kim GT (2013) Kip-related protein 3 is required for control of endoreduplication in the shoot apical meristem and leaves of Arabidopsis. Mol Cells **35:** 47–53

Kamura T, Hara T, Matsumoto M, Ishida N, Okumura F, Hatakeyama S, Yoshida M, Nakayama K, Nakayama KI (2004) Cytoplasmic ubiquitin ligase KPC regulates proteolysis of p27(Kip1) at G1 phase. Nat Cell Biol **6:** 1229–1235

Kitsios G, Doonan JH (2011) Cyclin dependent protein kinases and stress responses in plants. Plant Signal Behav **6:** 204–209

Komaki S, Sugimoto K (2012) Control of the plant cell cycle by developmental and environmental cues. Plant Cell Physiol **53:** 953–964

Kumar N, Harashima H, Kalve S, Bramsiepe J, Wang K, Sizani BL, Bertrand LL, Johnson MC, Faulk C, Dale R, et al (2015) Functional conservation in the SIAMESE-RELATED family of cyclin-dependent kinase inhibitors in land plants. Plant Cell **27:** 3065–3080

Kumar N, Larkin JC (2017) Why do plants need so many cyclin-dependent kinase inhibitors? Plant Signal Behav **12:** e1282021

Lechner E, Leonhardt N, Eisler H, Parmentier Y, Alioua M, Jacquet H, Leung J, Genschik P (2011) MATH/BTB CRL3 receptors target the homeodomain-leucine zipper ATHB6 to modulate abscisic acid signaling. Dev Cell **21:** 1116–1128

Leiva-Neto JT, Grafi G, Sabelli PA, Dante RA, Woo YM, Maddock S, Gordon-Kamm WJ, Larkins BA (2004) A dominant negative mutant of cyclin-dependent kinase A reduces endoreduplication but not cell size or gene expression in maize endosperm. Plant Cell **16:** 1854–1869

Liu J, Zhang Y, Qin G, Tsuge T, Sakaguchi N, Luo G, Sun K, Shi D, Aki S, Zheng N, et al (2008) Targeted degradation of the cyclin-dependent kinase inhibitor ICK4/KRP6 by RING-type E3 ligases is essential for mitotic cell cycle progression during Arabidopsis gametogenesis. Plant Cell **20:** 1538–1554

Ma X, Sukiran NL, Ma H, Su Z (2014) Moderate drought causes dramatic floral transcriptomic reprogramming to ensure successful reproductive development in Arabidopsis. BMC Plant Biol **14:** 164

Nakagami H, Kawamura K, Sugisaka K, Sekine M, Shinmyo A (2002) Phosphorylation of retinoblastoma-related protein by the cyclin D/cyclin-dependent kinase complex is activated at the G1/S-phase transition in tobacco. Plant Cell **14:** 1847–1857

Noir S, Marrocco K, Masoud K, Thomann A, Gusti A, Bitrian M, Schnittger A, Genschik P (2015) The control of *Arabidopsis thaliana*

growth by cell proliferation and endoreplication requires the F-box protein FBL17. Plant Cell **27:** 1461–1476

Nowack MK, Harashima H, Dissmeyer N, Zhao X, Bouyer D, Weimer AK, De Winter F, Yang F, Schnittger A (2012) Genetic framework of cyclin-dependent kinase function in Arabidopsis. Dev Cell **22:** 1030–1040

Peres A, Churchman ML, Hariharan S, Himanen K, Verkest A, Vandepoele K, Magyar Z, Hatzfeld Y, Van Der Schueren E, Beemster GT, et al (2007) Novel plant-specific cyclin-dependent kinase inhibitors induced by biotic and abiotic stresses. J Biol Chem **282:** 25588–25596

Plett JM, Williams M, LeClair G, Regan S, Beardmore T (2014) Heterologous over-expression of ACC SYNTHASE8 (ACS8) in *Populus tremula* x *P. alba* clone 717-1B4 results in elevated levels of ethylene and induces stem dwarfism and reduced leaf size through separate genetic pathways. Front Plant Sci **5:** 514

Ren H, Santner A, del Pozo JC, Murray JA, Estelle M (2008) Degradation of the cyclin-dependent kinase inhibitor KRP1 is regulated by two different ubiquitin E3 ligases. Plant J **53:** 705–716

Roeder AH, Chickarmane V, Cunha A, Obara B, Manjunath BS, Meyerowitz EM (2010) Variability in the control of cell division underlies sepal epidermal patterning in *Arabidopsis thaliana*. PLoS Biol **8:** e1000367

Rost B, Liu J (2003) The PredictProtein server. Nucleic Acids Res **31:** 3300–3304

Schnittger A, Weinl C, Bouyer D, Schöbinger U, Hülskamp M (2003) Misexpression of the cyclin-dependent kinase inhibitor ICK1/KRP1 in single-celled Arabidopsis trichomes reduces endoreduplication and cell size and induces cell death. Plant Cell **15:** 303–315

Seki M, Umezawa T, Urano K, Shinozaki K (2007) Regulatory metabolic networks in drought stress responses. Curr Opin Plant Biol **10:** 296–302

Sheaff RJ, Groudine M, Gordon M, Roberts JM, Clurman BE (1997) Cyclin E-CDK2 is a regulator of p27Kip1. Genes Dev **11:** 1464–1478

Shi J, Gao H, Wang H, Lafitte HR, Archibald RL, Yang M, Hakimi SM, Mo H, Habben JE (2017) ARGOS8 variants generated by CRISPR-Cas9 improve maize grain yield under field drought stress conditions. Plant Biotechnol J **15:** 207–216

Shi J, Habben JE, Archibald RL, Drummond BJ, Chamberlin MA, Williams RW, Lafitte HR, Weers BP (2015) Overexpression of ARGOS genes modifies plant sensitivity to ethylene, leading to improved drought tolerance in both Arabidopsis and maize. Plant Physiol **169:** 266–282

Skirycz A, Claeys H, De Bodt S, Oikawa A, Shinoda S, Andriankaja M, Maleux K, Eloy NB, Coppens F, Yoo SD, Saito K, Inzé D (2011a) Pause-and-stop: the effects of osmotic stress on cell proliferation during early leaf development in Arabidopsis and a role for ethylene signaling in cell cycle arrest. Plant Cell **23:** 1876–1888

Skirycz A, Vandenbroucke K, Clauw P, Maleux K, De Meyer B, Dhondt S, Pucci A, Gonzalez N, Hoeberichts F, Tognetti VB, et al (2011b) Survival and growth of Arabidopsis plants given limited water are not equal. Nat Biotechnol **29:** 212–214

Song J, Zhu C, Zhang X, Wen X, Liu L, Peng J, Guo H, Yi C (2015) Biochemical and structural insights into the mechanism of DNA recognition by Arabidopsis ETHYLENE INSENSITIVE3. PLoS One **10:** e0137439

Starostina NG, Kipreos ET (2012) Multiple degradation pathways regulate versatile CIP/KIP CDK inhibitors. Trends Cell Biol **22:** 33–41

Street IH, Aman S, Zubo Y, Ramzan A, Wang X, Shakeel SN, Kieber JJ, Schaller GE (2015) Ethylene inhibits cell proliferation of the Arabidopsis root meristem. Plant Physiol **169:** 338–350

Takatsuka H, Umeda-Hara C, Umeda M (2015) Cyclin-dependent kinase-activating kinases CDKD;1 and CDKD;3 are essential for preserving mitotic activity in *Arabidopsis thaliana*. Plant J **82:** 1004–1017

Tardieu F (2012) Any trait or trait-related allele can confer drought tolerance: just design the right drought scenario. J Exp Bot **63:** 25–31

Thomann A, Lechner E, Hansen M, Dumbliauskas E, Parmentier Y, Kieber J, Scheres B, Genschik P (2009) Arabidopsis CULLIN3 genes regulate primary root growth and patterning by ethylene-dependent and -independent mechanisms. PLoS Genet **5:** e1000328

Van Leene J, Hollunder J, Eeckhout D, Persiau G, Van De Slijke E, Stals H, Van Isterdael G, Verkest A, Neirynck S, Buffel Y, et al (2010) Targeted interactomics reveals a complex core cell cycle machinery in *Arabidopsis thaliana*. Mol Syst Biol **6:** 397

Verkest A, Manes CL, Vercruysse S, Maes S, Van Der Schueren E, Beeckman T, Genschik P, Kuiper M, Inzé D, De Veylder L (2005) The cyclin-dependent kinase inhibitor KRP2 controls the onset of the endoreduplication cycle during Arabidopsis leaf development through inhibition of mitotic CDKA;1 kinase complexes. Plant Cell **17:** 1723–1736

Verslues PE (2017) Time to grow: factors that control plant growth during mild to moderate drought stress. Plant Cell Environ **40:** 177–179

Vierstra RD (2009) The ubiquitin-26S proteasome system at the nexus of plant biology. Nat Rev Mol Cell Biol **10:** 385–397

Walker JD, Oppenheimer DG, Concienne J, Larkin JC (2000) SIAMESE, a gene controlling the endoreduplication cell cycle in *Arabidopsis thaliana* trichomes. Development **127:** 3931–3940

Wang H, Zhou Y, Gilmer S, Whitwill S, Fowke LC (2000) Expression of the plant cyclin-dependent kinase inhibitor ICK1 affects cell division, plant growth and morphology. Plant J **24:** 613–623

Weinl C, Marquardt S, Kuijt SJ, Nowack MK, Jakoby MJ, Hülskamp M, Schnittger A (2005) Novel functions of plant cyclin-dependent kinase inhibitors, ICK1/KRP1, can act non-cell-autonomously and inhibit entry into mitosis. Plant Cell **17:** 1704–1722

Wilkins O, Bräutigam K, Campbell MM (2010) Time of day shapes Arabidopsis drought transcriptomes. Plant J **63:** 715–727

Yang C, Li L (2017) Hormonal regulation in shade avoidance. Front Plant Sci **8:** 1527

Yi D, Alvim Kamei CL, Cools T, Vanderauwera S, Takahashi N, Okushima Y, Eekhout T, Yoshiyama KO, Larkin J, Van den Daele H, et al (2014) The Arabidopsis SIAMESE-RELATED cyclin-dependent kinase inhibitors SMR5 and SMR7 regulate the DNA damage checkpoint in response to reactive oxygen species. Plant Cell **26:** 296–309

Zhao L, Li Y, Xie Q, Wu Y (2017) Loss of CDKC;2 increases both cell division and drought tolerance in *Arabidopsis thaliana*. Plant J **91:** 816–828

Zhou Y, Li G, Brandizzi F, Fowke LC, Wang H (2003) The plant cyclin-dependent kinase inhibitor ICK1 has distinct functional domains for in vivo kinase inhibition, protein instability and nuclear localization. Plant J **35:** 476–489

Züst T, Agrawal AA (2017) Trade-offs between plant growth and defense against insect herbivory: an emerging mechanistic synthesis. Annu Rev Plant Biol **68:** 513–534